

# A Multivariate Spline based Collocation Method for Numerical Solution of Partial Differential Equations

Ming-Jun Lai\*

Jinsil Lee †

## Abstract

We propose a collocation method based on multivariate polynomial splines over triangulation or tetrahedralization for numerical solution of partial differential equations. We start with a detailed explanation of the method for the Poisson equation and then extend the study to the second order elliptic PDE in non-divergence form. We shall show that the numerical solution can approximate the exact PDE solution very well. Then we present a large amount of numerical experimental results to demonstrate the performance of the method over the 2D and 3D settings. In addition, we present a comparison with the existing multivariate spline methods in [1] and [11] to show that the new method produces a similar and sometimes more accurate approximation in a more efficient fashion.

## 1 Introduction

In this paper, we propose and study a new collocation method based on multivariate splines for numerical solution of partial differential equations over polygonal domain in  $\mathbb{R}^d$  for  $d \geq 2$ . Instead of using a second order elliptic equation in divergence form:

$$\begin{cases} -\sum_{i,j=1}^d \frac{\partial}{\partial x_i} (a^{ij}(x) \frac{\partial}{\partial x_j} u) + \sum_{i=1}^d b^i(x) \frac{\partial}{\partial x_i} u + c^1(x)u = f, & x \in \Omega \subset \mathbb{R}^d, \\ u = g, & \text{on } \partial\Omega \end{cases} \quad (1)$$

which is often used for various finite element methods, we discuss in this paper a more general form of second order elliptic PDE in non-divergence form:

$$\begin{cases} \sum_{i,j=1}^d a^{ij}(x) \frac{\partial}{\partial x_i} \frac{\partial}{\partial x_j} u + \sum_{i=1}^d b^i(x) \frac{\partial}{\partial x_i} u + c(x)u = f, & x \in \Omega \subset \mathbb{R}^d, \\ u = g, & \text{on } \partial\Omega, \end{cases} \quad (2)$$

where the PDE coefficient functions  $a^{ij}(x), i, j = 1, \dots, d$  are in  $L^\infty(\Omega)$  and satisfy the standard elliptic condition.

In addition, when  $d \geq 2$ , we shall assume the so-called Cordés condition, see (27) in a later section or see [18]. Numerical solutions to the 2nd order PDE in the non-divergence form have been studied extensively recently. See some studies in [18], [11], [15], [19], [17], and etc.. The method in this paper provides a new and more effective approach.

---

\*mjlai@uga.edu, Department of Mathematics, University of Georgia, Athens, GA 30602

†Jinsil.Lee@uga.edu, Department of Mathematics, University of Georgia, Athens, GA 30602

In this paper, we shall use the ideas of the classic collocation method to numerically solve (2) based on multivariate splines. We mainly use the Sobolev space  $H^2(\Omega)$ . It is known when  $\Omega$  is convex (cf. [5]), the solution to the Poisson equation with zero boundary condition, i.e.  $g = 0$  will be  $H^2(\Omega)$ . Recently, the researchers in [4] showed that when  $\Omega$  has an uniformly positive reach, the solution of (2) with zero boundary condition will be in  $H^2(\Omega)$ . Domains of uniformly positive reach, e.g. star-shaped domain and domains with holes are shown in [4]. See more examples in the next preliminary section. Many more domains than convex domains can have  $H^2$  solution. For any  $u \in H^2(\Omega)$ , we use the standard  $H^2$  norm

$$\|u\|_{H^2} = \|u\|_{L^2(\Omega)} + \|\nabla u\|_{L^2(\Omega)} + \sum_{i,j=1}^d \left\| \frac{\partial}{\partial x_i} \frac{\partial}{\partial x_j} u \right\|_{L^2(\Omega)} \quad (3)$$

for all  $u$  on  $H^2(\Omega)$  and the semi-norm

$$|u|_{H^2} = \sum_{i,j=1}^d \left\| \frac{\partial}{\partial x_i} \frac{\partial}{\partial x_j} u \right\|_{L^2(\Omega)}. \quad (4)$$

Since we will use multivariate spline functions to approximate the solution  $u \in H^2(\Omega)$ , we use  $C^r$  smooth spline functions with  $r \geq 1$  and the degree  $D$  of splines sufficiently large satisfying  $D \geq 3r + 2$  in  $\mathbb{R}^2$  and  $D \geq 6r + 3$  in  $\mathbb{R}^3$ . Let  $S_D^r(\Delta)$  be the spline space of degree  $D$  and smoothness  $r$  over triangulation or tetrahedralization  $\Delta$  of  $\Omega$ . How to use such spline functions has been explained in [13], [1], [16], and [17], and etc.. We shall give a preliminary on multivariate splines in the next section.

We now explain our spline based collocation method. For simplicity, we use the standard Poisson equation which is a special case of the PDE (2).

$$\begin{cases} -\Delta u = f, & \text{in } \Omega \subset \mathbb{R}^d, \\ u = g, & \text{on } \partial\Omega. \end{cases} \quad (5)$$

When  $\Omega$  has a uniform positive reach, the solution to the Poisson equation will be in  $H^2(\Omega)$ . We shall use  $C^r$  spline functions with  $r \geq 1$  to approximate the solution  $u$ . In addition, we shall use the so-called domain points (cf. [9] or next section) to be the collocation points. Letting  $\xi_i, i = 1, \dots, N$  be the domain points of  $\Delta$  and degree  $D' > 0$ , where  $D'$  will be different from  $D$ , our multivariate spline based collocation method is to seek a spline function  $s \in S_D^r(\Delta)$  satisfying

$$\begin{cases} -\Delta s(\xi_i) = f(\xi_i), & \xi_i \in \Omega \subset \mathbb{R}^d, i = 1, \dots, N, \\ s(\xi_i) = g(\xi_i), & \xi_i \in \partial\Omega, i = 1, \dots, N. \end{cases} \quad (6)$$

It is known a multivariate spline space is a linear vector space which is spanned by a set of basis functions. However, it is difficult to construct locally supported basis functions in  $C^r(\Omega)$  with  $r \geq 1$  due to the complication of the smoothness conditions over  $\Delta$ . Typically, any small perturbation of a vertex in  $\Delta$  may change the dimension of  $S_D^r(\Delta)$ . On the other hand, the smoothness conditions can be written as a system of linear equations, i.e.  $H\mathbf{c} = 0$ , where  $\mathbf{c}$  is the coefficient vector of spline function  $s \in S_D^r(\Delta)$  and  $H$  is the matrix consisting of all smoothness condition across each interior edge of  $\Delta$  (cf. [9] or next section). To overcome this difficulty, we will begin with a discontinuous spline space  $s \in S_D^{-1}(\Delta)$  and then add the smoothness conditions

$H\mathbf{c} = 0$ . One of the key ideas is to let a computer decide how to choose  $\mathbf{c}$  to satisfy  $H\mathbf{c} = 0$  and (6) above simultaneously. Clearly, (6) leads to a linear system which may not have a unique solution. It may be an over-determined linear system if  $D' > D$  or an under-determined linear system if  $D' < D$ . Our method is to use a least squares solution if the system is overdetermined or a sparse solution if the system is under-determined (cf. [12]).

To establish the convergence of the spline based collocation solution  $s$  as the size of  $\Delta$  goes to zero, we define a new norm  $\|u\|_L$  on  $H^2(\Omega) \cap H_0^1(\Omega)$  for the Poisson equation as follows.

$$\|u\|_L = \|\Delta u\|_{L^2(\Omega)}. \quad (7)$$

We mainly show that the new norm is equivalent to the standard norm on Banach space  $H^2(\Omega) \cap H_0^1(\Omega)$ . That is,

**Theorem 1** *Suppose  $\Omega \subset \mathbb{R}^d$  be a bounded domain and the closure of  $\Omega$  is of uniformly positive reach  $r_\Omega > 0$ . Then there exist two positive constants  $A$  and  $B$  such that*

$$A\|u\|_{H^2} \leq \|u\|_L \leq B\|u\|_{H^2}, \quad \forall u \in H^2(\Omega) \cap H_0^1(\Omega). \quad (8)$$

See the proof of Theorem 4 in a later section. Letting  $u \in H^2(\Omega) \cap H_0^1(\Omega)$  be the solution of (5) with  $g = 0$  and  $u_s$  be the spline solution of (6), we use the first inequality above to have

$$A\|u - u_s\|_{H^2} \leq \|u - u_s\|_L.$$

It can be seen from (6) that the first equation can be written as

$$\Delta(s(\xi_i) - u(\xi_i)), i = 1, \dots, N \quad (9)$$

which is a discretization of  $\|u - u_s\|_L^2$ . Let  $|\Delta|$  be the size of triangulation or tetrahedralization  $\Delta$ . Since we can use a spline function to approximate  $u$  if  $u$  is sufficiently smooth when the size  $|\Delta|$  goes to zero (cf. [9]), we seek the minimizer  $u_s$  of a minimization to be explained in a later section. Then the root mean square error (RMSE) will be small for a sufficiently large amount of collocation points and distributed evenly and the size  $|\Delta|$  of  $\Delta$  is small, our Theorem 1 implies that  $\|u - u_s\|_{H^2}$  is small. Furthermore, we will show

$$\|u - u_s\|_{L^2(\Omega)} \leq C|\Delta|^2\|u - u_s\|_L \text{ and } \|\nabla(u - u_s)\|_{L^2(\Omega)} \leq C|\Delta|\|u - u_s\|_L \quad (10)$$

for a positive constant  $C$ , under the assumption that  $u - u_s = 0$  on  $\partial\Omega$ . These will establish the multivariate spline based collocation method for the Poisson equation.

In general, we let  $\mathcal{L}$  be the PDE operator in (11). Note that we begin with the second order term of the PDE just for convenience.

$$\begin{cases} \sum_{i,j=1}^d a^{ij}(x) \frac{\partial}{\partial x_i} \frac{\partial}{\partial x_j} u = f, & x \in \Omega \subset \mathbb{R}^d, \\ u = g, & \text{on } \partial\Omega, \end{cases} \quad (11)$$

We shall similarly define a new norm associated with the PDE (11):

$$\|u\|_{\mathcal{L}} = \|\mathcal{L}(u)\|_{L^2(\Omega)}. \quad (12)$$

Similarly we will show the following.

**Theorem 2** *Suppose  $\Omega \subset \mathbb{R}^d$  be a bounded domain and the closure of  $\Omega$  is of uniformly positive reach  $r_\Omega > 0$ . Suppose that the second order partial differential equation in (11) is elliptic, i.e. satisfying (26) and satisfies the Cordés condition if  $d \geq 2$ . There exist two positive constants  $A_1$  and  $B_1$  such that*

$$A_1 \|u\|_{H^2} \leq \|u\|_{\mathcal{L}} \leq B_1 \|u\|_{H^2}, \quad \forall u \in H^2(\Omega) \cap H_0^1(\Omega). \quad (13)$$

See a proof in a section later. Similar to the Poisson equation setting, this result will enable us to establish the convergence of the spline based collocation method for the second order elliptic PDE in non-divergence form. Also, we will have the improved convergence similar to (10).

There are a few advantages of the collocation methods over the traditional finite element methods, discontinuous Galerkin methods, virtual element methods, and etc.. For example, no weak formulation of the PDE solution is required and hence, no numerical quadrature is needed for the computation. For another example, it is more flexible to deal with the discontinuity arising from the PDE coefficients as one may easily adjust the locations of some collocation points close to the both sides of discontinuous curves. A clear advantage of multivariate splines is that one can increase the accuracy of the approximation by increasing the degree of splines and/or the number of collocation points which can be cheaper than finding the solution over a uniform refinement of the underlying triangulation or tetrahedralization within the memory budget of a computer.

We shall provide many numerical results in 2D and 3D to demonstrate how well the spline based collocation methods can perform. Mainly, we would like to show the performance of solutions under the various settings: (1) the PDE coefficients are smooth or not very smooth, (2) the PDE solutions are smooth or not very smooth, (3) the domain of interest may not be uniformly positive reach, even very complicated domain such as the human head used in the numerical experiment in this paper, and (4) the dimension  $d$  can be 2 or 3. In particular, using splines of high degree enables us to find a numerical solution with high accuracy. We are not able to show the rate of convergence in terms of the size of triangulation. Instead, we present the accuracy of spline solutions for various kinds of testing functions. In addition, we shall compare with the existing methods in [1] and [11] to demonstrate that the multivariate spline based collocation method can be better in the sense that it is more accurate and more efficient under the assumption that the associated collocation matrices are generated beforehand. Finally, we remark that we have extended our study to the biharmonic equation, i.e. Stokes equations and Navier-Stokes equations as well as the Monge-Ampère equation. These will leave to a near future publication, e.g. [14].

## 2 Preliminaries on Domains of Positive Reach and Multivariate Splines

### 2.1 Domains with positive reach

Let us introduce a concept on domains of interest explained in [4].

**Definition 1** *Let  $K \subseteq \mathbb{R}^n$  be a non-empty set. Let  $r_K$  be the supremum of the number  $r$  such that every points in*

$$P = \{x \in \mathbb{R}^n : \text{dist}(x, K) < r\}$$

has a unique projection in  $K$ . The set  $K$  is said to have a positive reach if  $r_K > 0$ .

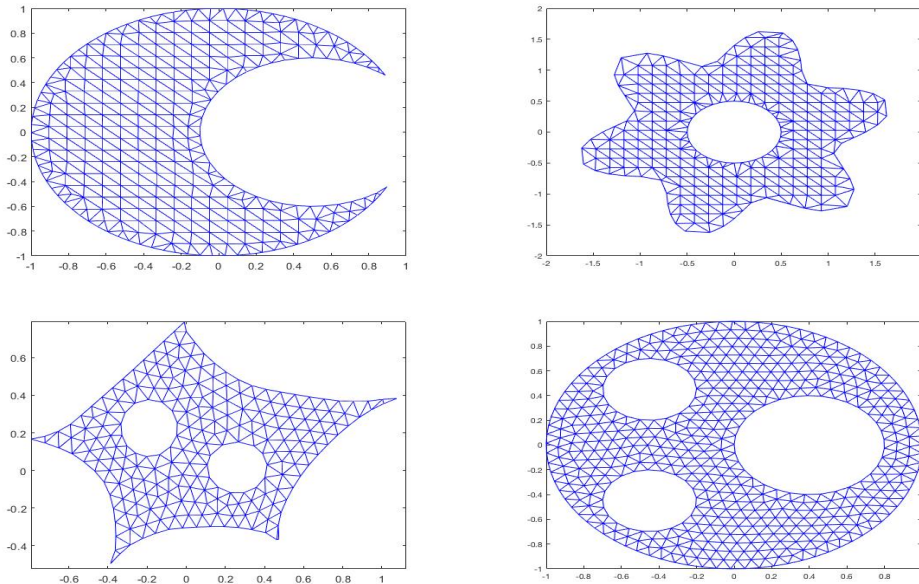


Figure 1: Domains with positive reach

A domain with  $C^2$  boundary has a positive reach. As Figure 1 illustrates, sets of positive reach are much more general than convex sets. See Figure 2 for domains with positive reach in the 3D setting. Let  $B(0, \epsilon)$  be the closed ball centering at 0 with radius  $\epsilon > 0$ , and let  $K^c$  stand for the complement of the set  $K \in \mathbb{R}^n$ . For any  $\epsilon > 0$ , the set

$$E_\epsilon(K) := (K^c + B(0, \epsilon))^c \subseteq K$$

is called an  $\epsilon$ -erosion of  $K$ .

**Definition 2** A set  $K \subseteq \mathbb{R}^n$  is said to have a uniformly positive reach  $r_0$  if there exists some  $\epsilon_0 > 0$  such that for all  $\epsilon \in [0, \epsilon_0]$ ,  $E_\epsilon(K)$  has a positive reach at least  $r_0$ .

And we have the following property about these domains

**Lemma 1** If  $\Omega \subset \mathbb{R}^n$  is of positive reach  $r_0$ , then for any  $0 < \epsilon < r_0$ , the boundary of  $\Omega_\epsilon := \Omega + B(0, \epsilon)$  containing  $\Omega$  is of  $C^{1,1}$ . Furthermore,  $\Omega_\epsilon$  has a positive reach  $\geq r_0 - \epsilon$ .

In [4], Gao and Lai proved the following regularity theorem

**Theorem 3** Let  $\Omega$  be a bounded domain. Suppose the closure of  $\Omega$  is of uniformly positive reach  $r_\Omega$ . For any  $f \in L^2(\Omega)$ , let  $u \in H_0^1(\Omega)$  be the unique weak solution of the Dirichlet problem:

$$\begin{cases} -\Delta u &= f \text{ in } \Omega \\ u &= 0 \text{ on } \partial\Omega \end{cases}$$

Then  $u \in H^2(\Omega)$  in the sense that

$$\sum_{i,j=1}^n \int_{\Omega} \left( \frac{\partial^2 u}{\partial x_i \partial x_j} \right)^2 \leq C_0 \int_{\Omega} f^2 dx$$

for a positive constant  $C_0$  depending only on  $r_{\Omega}$ .

## 2.2 Multivariate Splines

Next we quickly summarize the essentials of multivariate splines in this subsection. We introduce bivariate spline functions first. Before we start, we first review some facts about triangles. Given a triangle  $T$ , we write  $|T|$  for the length of its longest edge, and  $\rho_T$  for the radius of the largest disk that can be inscribed in  $T$ . For any polygonal domain  $\Omega \subset \mathbb{R}^d$  with  $d = 2$ , let  $\Delta := \{T_1, \dots, T_n\}$  be a triangulation of  $\Omega$  which is a collection of triangles and  $\mathcal{V}$  be the set of vertices of  $\Delta$ . We called a triangulation as a quasi-uniform triangulation if all triangles  $T$  in  $\Delta$  have comparable sizes in the sense that

$$\frac{|T|}{\rho_T} \leq C < \infty, \quad \text{all triangles } T \in \Delta,$$

where  $\rho_T$  is the inradius of  $T$ . Let  $|\Delta|$  be the length of the longest edge in  $\Delta$ . For a triangle  $T = (v_1, v_2, v_3) \in \Omega$ , we define the barycentric coordinates  $(b_1, b_2, b_3)$  of a point  $(x, y) \in \Omega$ . These coordinates are the solution to the following system of equations

$$\begin{aligned} b_1 + b_2 + b_3 &= 1 \\ b_1 v_{1,x} + b_2 v_{2,x} + b_3 v_{3,x} &= x \\ b_1 v_{1,y} + b_2 v_{2,y} + b_3 v_{3,y} &= y \end{aligned}$$

where the vertices  $v_i = (v_{i,x}, v_{i,y})$  for  $i = 1, 2, 3$  and are nonnegative if  $(x, y) \in T$ . We use the barycentric coordinates to define the Bernstein polynomials of degree  $D$ :

$$B_{i,j,k}^T(x, y) := \frac{D!}{i!j!k!} b_1^i b_2^j b_3^k, \quad i + j + k = D,$$

which form a basis for the space  $\mathcal{P}_D$  of polynomials of degree  $D$ . Therefore, we can represent all  $s \in \mathcal{P}_D$  in B-form:

$$s|_T = \sum_{i+j+k=D} c_{ijk} B_{ijk}^T, \quad \forall T \in \Delta,$$

where the B-coefficients  $c_{i,j,k}$  are uniquely determined by  $s$ .

Moreover, for given  $T = (v_1, v_2, v_3) \in \Delta$ , we define the associated set of domain points to be

$$\mathcal{D}_{D,T} := \left\{ \frac{iv_1 + jv_2 + kv_3}{D} \right\}_{i+j+k=D}. \quad (14)$$

Let  $\mathcal{D}_{D,\Delta} = \cup_{T \in \Delta} \mathcal{D}_{D,T}$  be the domain points of triangulation  $\Delta$  and degree  $D$ .

We use the discontinuous spline space  $S_D^{-1}(\Delta) := \{s|_T \in \mathcal{P}_D, T \in \Delta\}$  as a base. Then we add the smoothness conditions to define the space  $S_D^r := C^r(\Omega) \cap S_D^{-1}(\Delta)$ . The smoothness conditions are explained in [9]. Indeed, see Theorem 2.28 and 15.31 in [9]. Let  $\mathbf{c}$  be the coefficient

vector of  $s \in S_D^{-1}(\Delta)$  and  $H$  be the matrix which consists of the smoothness conditions across each interior edge of  $\Delta$ . It is known that  $H\mathbf{c} = 0$  if and only if  $s \in C^r(\Omega)$  (cf. [9]).

Computations involving splines written in B-form can be performed easily according to [13], [1] and [11]. In fact, these spline functions have numerically stable, closed-form formulas for differentiation, integration, and inner products. If  $D \geq 3r + 2$ , spline functions on quasi-uniform triangulations have optimal approximation power.

**Lemma 2** ([Lai and Schumaker, 2007[9]]) *Let  $k \geq 3r + 2$  with  $r \geq 1$ . Suppose  $\Delta$  is a quasi-uniform triangulation of  $\Omega$ . Then for every  $u \in W_q^{k+1}(\Omega)$ , there exists a quasi-interpolatory spline  $s_u \in \mathcal{S}_k^r(\Delta)$  such that*

$$\|D_x^\alpha D_y^\beta (u - s_u)\|_{q,\Omega} \leq C|\Delta|^{k+1-\alpha-\beta}|u|_{k+1,q,\Omega}$$

for a positive constant  $C$  dependent on  $u, r, k$  and the smallest angle of  $\Delta$ , and for all  $0 \leq \alpha + \beta \leq k$  with

$$|u|_{k,q,\Omega} := \left( \sum_{a+b=k} \|D_x^a D_y^b u\|_{L^q(\Omega)}^q \right)^{\frac{1}{q}}.$$

Similarly, for trivariate splines, let  $\Omega \subset \mathbb{R}^3$  and  $\Delta$  be a tetrahedralization of  $\Omega$ . We define a trivariate spline just like bivariate splines by using Bernstein-Bézier polynomials defined on each tetrahedron  $t \in \Delta$ . Letting

$$\mathcal{S}_D^r(\Delta) = \{s \in C^r(\Omega) : s|_t \in \mathbb{P}_D, t \in \Delta\} = C^r(\Omega) \cap S_D^{-1}(\Delta)$$

be the spline space of degree  $D$  and smoothness  $r \geq 0$ , each  $s \in \mathcal{S}_D^r(\Delta)$  can be rewritten as

$$s|_t = \sum_{i+j+k+\ell=D} c_{ijkl}^t B_{ijkl}^t, \quad \forall t \in \Delta,$$

where  $B_{ijkl}^t$  are Bernstein-Bézier polynomials (cf. [1], [9], [16]) which are nonzero on  $t$  and zero otherwise. Approximation properties of trivariate splines can be found in [10] and [7].

How to use them to solve partial differential equations based on the weak formulation like the finite element method has been discussed in [1], [16], [11].

### 3 A Spline Based Collocation Method for the Poisson Equation

For convenience, we simply explain our method when  $d = 2$  in this section. Numerical results in the settings of  $d = 2$  and  $d = 3$  will be given in later sections.

For a given  $\Delta$  triangulation, we use a spline space  $\mathcal{S}_D^r(\Delta)$  to find the coefficient vector  $\mathbf{c}$  of spline function  $s = \sum_{t \in \Delta} \sum_{i+j+k=D} c_{ijk}^t B_{ijk}^t \in \mathcal{S}_D^r(\Delta)$  satisfying the following equations

$$\begin{cases} -\sum_{t \in \Delta} \sum_{i+j+k=D} c_{ijk}^t \Delta B_{ijk}^t(\xi_i) = f(\xi_i), & \xi_i \in \Omega \subset \mathbb{R}^2 \\ s(\xi_i) = g(\xi_i), & \text{on } \partial\Omega, \end{cases} \quad (15)$$

where  $\{\xi_i\}_{i=1,\dots,N} \in \mathcal{D}_{D',\Delta}$  are the domain points of  $\Delta$  of degree  $D'$  as explained in (14) in the previous section and  $D' > D$ . Using these points, we have the following matrix equation:

$$-K\mathbf{c} := [-\Delta(B_{ijk}^t(\xi_i))] \mathbf{c} = [f(\xi_i)] = \mathbf{f},$$

where  $\mathbf{c}$  is the vector consisting of all spline coefficients  $c_{ijk}^t, i + j + k = D, t \in \Delta$ . In general, the spline  $s$  with coefficients in  $\mathbf{c}$  is a discontinuous function. In order to make  $s \in \mathcal{S}_D^r(\Delta)$ , its coefficient vector  $\mathbf{c}$  must satisfy the constraints  $H\mathbf{c} = 0$  for the smoothness conditions that the  $\mathcal{S}_D^r(\Delta)$  functions possess (cf. [9]).

Based on the smoothness conditions (cf. Theorem 2.28 or Theorem 15.38 in [9]), we can construct matrices  $H_0$  for the  $C^0$  smoothness conditions of spline functions and  $H_r$  for the  $C^r$  smoothness conditions, respectively. Our collocation method is to find  $\mathbf{c}^*$  by solving the following constrained minimization:

$$\min_{\mathbf{c}} J(\mathbf{c}) = \frac{1}{2}(\alpha\|B\mathbf{c} - \mathbf{g}\|^2 + \beta\|H\mathbf{c}\|^2 + \gamma\|H_0\mathbf{c}\|^2) \quad \text{subject to } \|K\mathbf{c} + \mathbf{f}\| \leq \epsilon_1, \quad (16)$$

where  $B, \mathbf{g}$  are associated with the boundary condition,  $H_r$  is associated with the smoothness condition with  $r = 2$  and  $H_0$  is associated with the smoothness condition with  $r = 0$ ,  $\alpha > 0, \beta > 0, \gamma > 0$  are fixed parameters, and  $\epsilon_1 > 0$  is a given tolerance. It is easy to see that the minimization (16) is a convex minimization problem over a convex feasible set. The problem (16) will have a unique solution. We shall use the following iterative method to solve the minimization problem (16). See Appendix for a derivation and a proof of the convergence.

---

**Algorithm 1:** Iterative Method

---

Let  $I$  be the identity matrix of  $\mathbb{R}^m$ . Fix  $\epsilon > 0$ . Given an initial guess  $\lambda^{(0)} \in \text{Im}(K)$ , we first compute

$$\mathbf{z}^{(1)} = (\alpha B^\top B + \beta H^\top H + \frac{1}{\epsilon} K^\top K)^{-1} (\alpha B^\top \mathbf{g} + \frac{1}{\epsilon} K^\top \mathbf{f} - K^\top \lambda^{(0)})$$

and iteratively compute

$$(\alpha B^\top B + \beta H^\top H + \frac{1}{\epsilon} K^\top K) \mathbf{z}^{(k+1)} = (\alpha B^\top B + \beta H^\top H) \mathbf{z}^{(k)} + \frac{1}{\epsilon} K^\top \mathbf{f}$$

for  $k = 1, 2, \dots$ , where  $\text{Im}(K)$  is the range of  $K$ .

---

Let  $u_s$  be the solution of Algorithm 1. We would like to show

$$\|u - u_s\|_{L^2(\Omega)} \leq C|\Delta|^2 \epsilon_1 \quad (17)$$

for some constant  $C > 0$ , where  $|\Delta|$  is the size of the underlying triangulation or tetrahedralization  $\Delta$  of the domain  $\Omega$ . To do so, we first show

**Lemma 3** *Suppose that  $\Omega$  is a polygonal domain. Suppose that  $u \in H^3(\Omega)$ . Then there exists a positive constant  $\hat{C}$  depending on  $D \geq 1$  and  $D' > D$  such that*

$$\|\Delta u(x, y) - \Delta u_s(x, y)\|_{L^2(\Omega)} \leq \epsilon_1 \hat{C}.$$



*Proof.* Indeed, by Lemma 2, we have a quasi-interpolatory spline  $s_u$  satisfying

$$|\Delta u(x, y) - \Delta s_u(x, y)| \leq \epsilon_1, \forall (x, y) \in \Omega$$

for a triangulation  $\Delta$  with  $|\Delta|$  small enough. Then, we use the minimization (16) to have the minimizer  $u_s$  satisfying

$$|\Delta u(x_i, y_i) - \Delta u_s(x_i, y_i)| \leq \epsilon_1$$

with sufficiently small  $|\Delta|$  for any domain points  $(x_i, y_i)$  which construct the collocation matrix  $K$ . Now, these two inequalities imply that

$$|\Delta u_s(x_i, y_i) - \Delta s_u(x_i, y_i)| \leq \epsilon_1 + \epsilon_1.$$

Note that  $\Delta u_s - \Delta s_u$  is a polynomial over each triangle  $t \in \Delta$  which has small values at the domain points. This implies that the polynomial  $\Delta u_s - \Delta s_u$  is small over  $t$ . That is,

$$|\Delta u_s(x, y) - \Delta s_u(x, y)| \leq C(\epsilon_1 + \epsilon_1) = 2C\epsilon_1 \quad (18)$$

by using Theorem 2.27 in [9]. Finally, we can use (18) to prove

$$|\Delta u(x, y) - \Delta u_s(x, y)| = |\Delta u(x, y) - \Delta s_u(x, y) + \Delta s_u(x, y) - \Delta u_s(x, y)| \leq \epsilon_1 + 2C\epsilon_1.$$

and then

$$\|\Delta u(x, y) - \Delta u_s(x, y)\|_{L^2(\Omega)} \leq \epsilon_1 \hat{C}$$

for a constant  $\hat{C}$  depending on the bounded domain  $\Omega$  and  $D, D'$ , but independent of  $|\Delta|$ .  $\square$

Now, let us consider the convergence of our method. Without loss of generality, we may assume  $g = 0$ . Indeed, for any general  $g$ , let  $u_g \in H^2(\Omega)$  be a function satisfying the boundary condition, i.e.  $u_g|_{\partial\Omega} = g$  and we consider the Poisson equation with solution  $w = u - u_g$  and the new right-hand side  $f_w = f + \Delta u_g$ . Recall the standard norm on  $H^2(\Omega)$  defined in (3). It is also a norm of  $H^2(\Omega) \cap H_0^1(\Omega)$ . It is easy to see that the space  $H^2(\Omega) \cap H_0^1(\Omega)$  is a Banach space with the norm  $\|\cdot\|_{H^2(\Omega)}$ . In addition, let us define a new norm  $\|u\|_L$  on  $H^2(\Omega) \cap H_0^1(\Omega)$  as follows.

$$\|u\|_L = \|\Delta u\|_{L^2(\Omega)} \quad (19)$$

We can easily show that  $\|\cdot\|_L$  is a norm on  $H^2(\Omega) \cap H_0^1(\Omega)$  as follows: Indeed, if  $\|u\|_L = 0$ , then  $\Delta u = 0$  in  $\Omega$  and  $u = 0$  on the boundary  $\partial\Omega$ . By the Green theorem, we get

$$\int_{\Omega} |\nabla u|^2 = - \int_{\Omega} u \Delta u + \int_{\partial\Omega} u \frac{\partial u}{\partial n} = 0.$$

By Poincaré's inequality, we get

$$\|u\|_{L^2(\Omega)} \leq C \|\nabla u\|_{L^2(\Omega)} = 0.$$

Hence, we know that  $u = 0$ . Next for any scalar  $a$ , it is trivial to have

$$\|au\|_L = \|\Delta au\|_{L^2(\Omega)} = |a| \|\Delta u\|_{L^2(\Omega)}.$$

Finally, the triangular inequality is also trivial.

$$\|u + v\|_L = \|\Delta(u + v)\|_{L^2(\Omega)} \leq \|u\|_L + \|v\|_L$$

by linearity of the Laplacian operator.

We now show that the new norm is equivalent to the standard norm on  $H^2(\Omega) \cap H_0^1(\Omega)$ . Indeed, recall a well-known property about the norm equivalence.

**Lemma 4** ([Brezis, 2011 [2]]) *Let  $E$  be a vector space equipped with two norms,  $\|\cdot\|_1$  and  $\|\cdot\|_2$ . Assume that  $E$  is a Banach space for both norms and that there exists a constant  $C > 0$  such that*

$$\|x\|_2 \leq C\|x\|_1, \quad \forall x \in E. \quad (20)$$

*Then the two norms are equivalent, i.e., there is a constant  $c > 0$  such that*

$$\|x\|_1 \leq c_1\|x\|_2, \quad \forall x \in E.$$

*Proof.* We define  $E_1 = (E, \|\cdot\|_1)$  and  $E_2 = (E, \|\cdot\|_2)$  be two spaces equipped with two different norms. It is easy to see that  $E_1$  and  $E_2$  are Banach spaces. Let  $I$  be the identity operator which maps any  $u$  in  $E_1$  to  $u$  in  $E_2$ . Clearly, it is an injection and onto because of the identity mapping and hence, it is a surjection. Because of (20), the mapping  $I$  is a continuous operator. Now we can use the well-known open mapping theorem. Let  $B_1(0, 1) = \{u \in E_1, \|u\|_1 \leq 1\}$  be an open ball. The open mapping theorem says that  $I(B_1(0, 1))$  is open and hence, it contains a ball  $B_2(0, c) = \{u \in E_2, \|u\|_2 < c\}$ . That is,  $B_2(0, c) \subset I(B_1(0, 1))$ . Let us claim that  $c\|u\|_1 \leq \|I(u)\|_2$  for all  $u \in E_1$ . Otherwise, there exists a  $u^*$  such that  $c\|u^*\|_1 > \|I(u^*)\|_2$ . That is,  $c > \|I(u^*/\|u^*\|_1)\|_2$ . So  $I(u^*/\|u^*\|_1) \in B_2(0, c)$ . There is a  $u^{**} \in B_1(0, 1)$  such that  $Iu^{**} = I(u^*/\|u^*\|_1)$ . Since  $I$  is an injection,  $u^{**} = I(u^*/\|u^*\|_1)$ . Since  $u^{**} \in B_1(0, 1)$ , we have  $1 > \|u^{**}\|_1 = \|(u^*/\|u^*\|_1)\|_1 = 1$  which is a contradiction. This shows that the claim is correct. we have thus  $c\|u\|_1 \leq \|I(u)\|_2 = \|u\|_2$  for all  $u \in E_1$ . We choose  $c_1 = 1/c$  to finish the proof.  $\square$

We are now ready to establish the following

**Theorem 4** *Suppose  $\Omega \subset \mathbb{R}^d$  be a bounded domain and the closure of  $\Omega$  is of uniformly positive reach  $r_\Omega > 0$ . There exist two positive constants  $A$  and  $B$  such that*

$$A\|u\|_{H^2} \leq \|u\|_L \leq B\|u\|_{H^2}, \quad \forall u \in H^2(\Omega) \cap H_0^1(\Omega). \quad (21)$$

*Proof.* We first show that  $H^2(\Omega) \cap H_0^1(\Omega)$  is the Banach space with the norm  $\|u\|_L$ . Assume that  $\{\Delta u_n\}$  is the Cauchy sequence in  $H^2(\Omega) \cap H_0^1(\Omega)$ . Then there exists  $\Delta u^* \in L^2(\Omega)$  such that  $\Delta u_n$  converges to  $\Delta u^*$ . Since there exist a unique  $u^*$  satisfying the Dirichlet problem:

$$\begin{cases} \Delta u &= \Delta u^* \\ u &= 0, \end{cases}$$

we can say that there exist the unique  $u^* \in H^2(\Omega) \cap H_0^1(\Omega)$  satisfying  $\|u_n - u^*\|_L \rightarrow 0$  as  $n \rightarrow \infty$  by Theorem 3. It is easy to show the inequality (20) from the fact that

$$\|u\|_L \leq \|\Delta u\|_{L^2(\Omega)} \leq \sum_{i,j=1}^d \left\| \frac{\partial^2}{\partial x_i \partial x_j} u \right\|_{L^2(\Omega)} \leq \|u\|_{H^2} \quad (22)$$

for all  $u \in H^2(\Omega) \cap H_0^1(\Omega)$ . We then use Lemma 4 to finish the proof. Indeed, by Lemma 4 and the above inequality, there exist  $\alpha > 0$  satisfying

$$\|u\|_{H^2} \leq \alpha \|u\|_L.$$

Therefore, we choose  $A = \frac{1}{\alpha}$  to finish the proof.  $\square$

Using Theorem 4, we immediately obtain the following theorem

**Theorem 5** *Suppose  $f$  and  $g$  are continuous over bounded domain  $\Omega \subseteq \mathbb{R}^d$  for  $d \geq 2$ . Suppose  $\Omega \subset \mathbb{R}^d$  be a bounded domain and the closure of  $\Omega$  is of uniformly positive reach  $r_\Omega > 0$ . Suppose that  $u \in H^3(\Omega)$  and  $(u - u_s)|_{\partial\Omega} = 0$ . We have the following inequality*

$$\|u - u_s\|_{L^2(\Omega)} \leq C\epsilon_1, \|\nabla(u - u_s)\|_{L^2(\Omega)} \leq C\epsilon_1$$

and

$$\sum_{i+j=2} \left\| \frac{\partial^2}{\partial x^i \partial y^j} u \right\|_{L^2(\Omega)} \leq C\epsilon_1$$

for a positive constant  $C$  depending on  $A$  and  $\Omega$ , where  $A$  is one of the constants in Theorem 4.

*Proof.* Using Lemma 3 and the assumption on the approximation on the boundary, we have

$$\|u - u_s\|_{H^2(\Omega)} \leq \frac{1}{A} \|\Delta(u - u_s)\|_{L^2(\Omega)} \leq \frac{1}{A} \epsilon_1 \hat{C}.$$

We choose  $C = \frac{\hat{C}}{A}$  to finish the proof.  $\square$

Finally we show that the convergence of  $\|u - u_s\|_{L^2(\Omega)}$  and  $\|\nabla(u - u_s)\|_{L^2(\Omega)}$  can be better

**Theorem 6** *Suppose that  $(u - u_s)|_{\partial\Omega} = 0$ . Under the assumptions in Theorem 5, we have the following inequality*

$$\|u - u_s\|_{L^2(\Omega)} \leq C|\Delta|^2\epsilon_1 \text{ and } \|\nabla(u - u_s)\|_{L^2(\Omega)} \leq C|\Delta|\epsilon_1$$

for a positive constant  $C = 1/A$ , where  $A$  is one of the constants in Theorem 4 and  $|\Delta|$  is the size of the underlying triangulation  $\Delta$ .

*Proof.* First of all, it is known for any  $w \in H^2(\Omega) \cap H_0^1(\Omega)$ , there is a continuous linear spline  $L_w$  over the triangulation  $\Delta$  such that

$$\|D_x^\alpha D_y^\beta (w - L_w)\|_{L^2(\Omega)} \leq C|\Delta|^{2-\alpha-\beta} |w|_{H^2(\Omega)} \quad (23)$$

for nonnegative integers  $\alpha \geq 0, \beta \geq 0$  and  $\alpha + \beta \leq 2$ , where  $|w|_{H^2(\Omega)}$  is the semi-norm of  $w$  in  $H^2(\Omega)$ . Indeed, we can use the same construction method for quasi-interpolatory splines used for the proof of Lemma 2 to establish the above estimate. The above estimate will be used twice below.

By the assumption that  $u - u_s = 0$  on  $\partial\Omega$ , it is easy to see

$$\|\nabla(u - u_s)\|_{L^2(\Omega)}^2 = - \int_{\Omega} \Delta(u - u_s)(u - u_s) = - \int_{\Omega} \Delta(u - u_s - L_{u-u_s})(u - u_s)$$

$$\begin{aligned}
&= \int_{\Omega} \nabla(u - u_s - L_{u-u_s}) \nabla(u - u_s) \leq \|\nabla(u - u_s)\|_{L^2(\Omega)} \|\nabla(u - u_s - L_{u-u_s})\|_{L^2(\Omega)} \\
&\leq \|\nabla(u - u_s)\|_{L^2(\Omega)} C|\Delta| \cdot \|u - u_s\|_{H^2(\Omega)} \\
&\leq \|\nabla(u - u_s)\|_{L^2(\Omega)} |\Delta| \frac{C}{A} \|\Delta(u - u_s)\|_{L^2(\Omega)}.
\end{aligned}$$

where we have used the first inequality in Theorem 4. It follows that  $\|\nabla(u - u_s)\|_{L^2(\Omega)} \leq |\Delta| \frac{C}{A} \epsilon_1$ .

Next we let  $w \in H^2(\Omega) \cap H_0^1(\Omega)$  be the solution to the following Poisson equation:

$$\begin{cases} -\Delta w = u - u_s & \text{in } \Omega \subset \mathbb{R}^d \\ w = 0 & \text{on } \partial\Omega, \end{cases} \quad (24)$$

Then we use the continuous linear spline  $L_w$  to have

$$\begin{aligned}
\|u - u_s\|_{L^2(\Omega)}^2 &= - \int_{\Omega} \Delta w (u - u_s) = - \int_{\Omega} \Delta(w - L_w)(u - u_s) \\
&= \int_{\Omega} \nabla(w - L_w) \nabla(u - u_s) \leq \|\nabla(u - u_s)\|_{L^2(\Omega)} \|\nabla(w - L_w)\|_{L^2(\Omega)} \\
&\leq \|\nabla(u - u_s)\|_{L^2(\Omega)} C|\Delta| \cdot \|w\|_{H^2(\Omega)} \leq \frac{C}{A} |\Delta| \epsilon_1 |\Delta| \frac{C}{A} \|\Delta w\|_{L^2(\Omega)} \\
&= \frac{C}{A} |\Delta| \epsilon_1 |\Delta| \frac{C}{A} \|u - u_s\|_{L^2(\Omega)}.
\end{aligned}$$

where we have used the first inequality in Theorem 4 and the estimate of  $\|\nabla(u - u_s)\|_{L^2(\Omega)}$  above. Hence, we have  $\|u - u_s\|_{L^2(\Omega)} \leq \frac{C^2}{A^2} |\Delta|^2 \epsilon_1$  as  $|\Delta| \rightarrow 0$ .  $\square$

## 4 General Second Order Elliptic Equations

Next we consider a collocation method based on bivariate/trivariate splines for a solution of the general second order elliptic equation in (2). For the PDE coefficient functions  $a^{ij}, b^i, c^1 \in L^\infty(\Omega)$ , we assume that

$$a_{ij} = a_{ji} \in L^\infty(\Omega) \quad \forall i, j = 1, \dots, d \quad (25)$$

and there exist  $\lambda, \Lambda$  such that

$$\lambda \sum_{i=1}^d \eta_i^2 \leq \sum_{i,j} a^{ij}(x) \eta_i \eta_j \leq \Lambda \sum_{i=1}^d \eta_i^2, \quad \forall \eta \in \mathbb{R}^d \setminus \{0\} \quad (26)$$

for all  $i, j$  and  $x \in \Omega$ . For convenience, we first assume that  $b^i = 0$  and  $c^1 = 0$ . In addition to the elliptic condition, we add the Cordés condition for well-posedness of the problem. We assume that there is an  $\epsilon \in (0, 1]$  such that

$$\frac{\sum_{i,j=1}^d (a^{i,j})^2}{(\sum_{i=1}^d a^{ii})^2} \leq \frac{1}{d-1+\epsilon} \quad \text{a.e. in } \Omega \quad (27)$$

Let  $\theta \in L^\infty(\Omega)$  be defined by

$$\theta := \frac{\sum_{i=1}^d a^{ii}}{\sum_{i,j=1}^d (a^{i,j})^2}.$$

Under these conditions, the researchers in [18] proved the following lemma

**Lemma 5** *Let the operator  $\mathcal{L}_1(u) := \sum_{i,j=1}^d a^{ij}(x) \frac{\partial^2}{\partial x_i \partial x_j} u$  satisfy (25), (26) and (27). Then for any open set  $U \subseteq \Omega$  and  $v \in H^2(U)$ , we have*

$$|\theta \mathcal{L}_1 v - \Delta v| \leq \sqrt{1-\epsilon} |D^2 v| \quad \text{a.e. in } U, \quad (28)$$

where  $\epsilon \in (0, 1]$  is as in (27).

Instead of using the convexity to ensure the existence of the strong solution of (2) in [18], we shall use the concept of uniformly positive reach in [4]. The following is just the restatement of Theorem 3.3 in [4].

**Theorem 7** *Suppose that  $\Omega \subset \mathbb{R}^d$  with  $d \geq 2$  is a bounded domain with uniformly positive reach. Then the second order elliptic PDE in (2) satisfying (27) has a unique strong solution in  $H^2(\Omega)$ .*

We now extend the collocation method in the previous section to find a numerical solution of (2). Similar to the discussion in the previous section, we can construct the following matrix for the PDE in (2):

$$\mathcal{K} := \left[ \sum_{i,j=1}^d a^{ij}(\xi_i) \frac{\partial^2}{\partial x_i \partial x_j} (B_{ijk}^t(\xi_i)) \right].$$

Similar to (16), consider the following minimization problem:

$$\min_{\mathbf{c}} J(\mathbf{c}) = \frac{1}{2} (\alpha \|\mathbf{B}\mathbf{c} - \mathbf{g}\|^2 + \beta \|\mathbf{H}\mathbf{c}\|^2 + \gamma \|\mathbf{H}_0\mathbf{c}\|^2) \quad \text{subject to } -\mathcal{K}\mathbf{c} = \mathbf{f}, \quad (29)$$

Again we will solve a nearby minimization problem as in the previous section. Just like the Poisson equation, we let  $\epsilon_1 = \min_{\mathbf{c}} \|\mathcal{K}\mathbf{c} + \mathbf{f}\|$  be the minimal value of (29). To study the convergence, we may assume that  $g = 0$  as in the previous section so that the solution  $u_s$  for (29) satisfies  $u_s = 0$  on  $\partial\Omega$  and hence,  $\|u - u_s\|_{L^2(\partial\Omega)} = 0$ . Also, since  $\epsilon_1 = \min_{\mathbf{c}} \|\mathcal{K}\mathbf{c} + \mathbf{f}\|$ , we may assume that  $\|\mathcal{L}u_s + f\|_{L^2(\Omega)} \leq \epsilon_1$ .

To show  $u_s$  approximate  $u$  over  $\Omega$ , let us define a new norm  $\|u\|_{\mathcal{L}}$  on  $H^2(\Omega) \cap H_0^1(\Omega)$  as follows.

$$\|u\|_{\mathcal{L}} = \|\mathcal{L}u\|_{L^2(\Omega)} \quad (30)$$

We can show that  $\|\cdot\|_{\mathcal{L}}$  is a norm on  $H^2(\Omega) \cap H_0^1(\Omega)$  as follows if  $\epsilon \in (0, 1]$  is large enough. Indeed, if  $\|u\|_{\mathcal{L}} = 0$ , then  $\mathcal{L}u = 0$  in  $\Omega$  and  $u = 0$  on the boundary  $\partial\Omega$ . Using this Lemma 5 and Theorem 4, we get

$$\int_{\Omega} \Delta u \Delta u - \int_{\Omega} (\Delta - \theta \mathcal{L})u \Delta u = \int_{\Omega} \theta \mathcal{L}(u) \Delta u = 0 \quad (31)$$

and

$$\begin{aligned} \int_{\Omega} \Delta u \Delta u - \int_{\Omega} (\Delta - \theta \mathcal{L})u \Delta u &\geq \int_{\Omega} |\Delta u|^2 - \int_{\Omega} \sqrt{1-\epsilon} |D^2 u| \cdot |\Delta u| \\ &= \int_{\Omega} |\Delta u|^2 - \int_{\Omega} \sqrt{1-\epsilon} |D^2 u| \cdot |\Delta u| \geq \|\Delta u\|^2 - \frac{\sqrt{1-\epsilon}}{A} \|\Delta u\| \|\Delta u\|. \end{aligned}$$

Therefore, if  $\epsilon > 1 - A^2$ , then

$$\left(1 - \frac{\sqrt{1-\epsilon}}{A}\right) \|\Delta u\| \leq 0.$$

Hence, we know that  $u = 0$ . The other two properties of the norm can be proved easily.

We mainly show that the above norm is equivalent to the standard norm on  $H^2(\Omega) \cap H_0^1(\Omega)$ .

**Theorem 8** Suppose that  $\Omega$  is bounded and has uniformly positive reach  $r_\Omega > 0$ . Then there exist two positive constants  $A_1$  and  $B_1$  such that

$$A_1 \|u\|_{H^2(\Omega)} \leq \|u\|_{\mathcal{L}} \leq B_1 \|u\|_{H^2(\Omega)}, \quad \forall u \in H^2(\Omega) \cap H_0^1(\Omega). \quad (32)$$

*Proof.* It follows that

$$\|u\|_{\mathcal{L}} \leq \max_{i,j=1,\dots,d} \|a^{ij}\|_\infty \sum_{i,j=1}^d \left\| \frac{\partial^2}{\partial x_i \partial x_j} u \right\|_{L^2(\Omega)} \leq B_1 \|u\|_{H^2(\Omega)}$$

for all  $u \in H^2(\Omega) \cap H_0^1(\Omega)$ , where  $B_1$  depending on  $d, \Lambda$  and  $C$ . Using Lemma 4 and the above inequality, there exist  $\alpha_1 > 0$  satisfying

$$\|u\|_{H^2} \leq \alpha_1 \|u\|_{\mathcal{L}}.$$

Therefore, we choose  $A_1 = \frac{1}{\alpha_1}$  to finish the proof.  $\square$

**Theorem 9** Let  $\Omega$  be a bounded and closed set satisfying the uniformly positive reach condition. Assume that  $a^{ij} \in L^\infty(\Omega)$  satisfy (25), (26) and (27) and  $\epsilon > 1 - A^2$ . Suppose that  $u \in H^3(\Omega)$  and  $u - u_s = 0$  on  $\partial\Omega$ . For the solution  $u$  of equation (11) and the corresponding minimizer  $u_s$ , we have the following inequality

$$\|u - u_s\|_{L^2(\Omega)} \leq C\epsilon_1$$

for a positive constant  $C$  depending on  $\Omega$  and  $A_1$  which is one of the constants in Theorem 8. Similar for  $\|\nabla(u - u_s)\|_{L^2(\Omega)}$  and  $|u - u_s|_{H^2}$ .

Next we consider the case that  $b^i$  and  $c^1$  are not zero. Assume that  $\|a^{ij}\|_\infty, \|b^i\|_\infty, \|c^1\|_\infty \leq \Lambda_1$  and we denote that  $\mathcal{L}_1(u) := \sum_{i,j=1}^d a^{ij}(x) \frac{\partial^2}{\partial x_i \partial x_j} u + \sum_{i=1}^d b^i(x) \frac{\partial}{\partial x_i} u + c^1(x)u$  and define a new norm  $\|u\|_{\mathcal{L}_1}$  on  $H^2(\Omega) \cap H_0^1(\Omega)$  as follows.

$$\|u\|_{\mathcal{L}_1} = \|\mathcal{L}_1 u\|_{L^2(\Omega)}. \quad (33)$$

Assume that  $\|u\|_{\mathcal{L}_1} = 0$ , i.e.,  $\mathcal{L}_1 u = 0$  over  $\Omega$  and  $u = 0$  on  $\partial\Omega$ . From (28), we have

$$\int_{\Omega} \theta \mathcal{L}(u) \Delta u \geq \|\Delta u\|^2 - \frac{\sqrt{1-\epsilon}}{A} \|\Delta u\|^2.$$

Then by the above inequality we get

$$\begin{aligned} 0 &= \int_{\Omega} \theta \mathcal{L}_1(u) \Delta u = \int_{\Omega} \theta \mathcal{L}(u) \Delta u + \sum_{i=1}^d \theta b^i(x) \frac{\partial}{\partial x_i} u \Delta u + \theta c^1(x) u \Delta u \\ &\geq \|\Delta u\|^2 - \frac{\sqrt{1-\epsilon}}{A} \|\Delta u\|^2 + \int_{\Omega} \sum_{i=1}^d \theta b^i(x) \frac{\partial}{\partial x_i} u \Delta u + \theta c^1(x) u \Delta u \\ &\geq \|\Delta u\|_{L^2(\Omega)}^2 - \frac{\sqrt{1-\epsilon}}{A} \|\Delta u\|_{L^2(\Omega)}^2 - \|\theta\|_\infty \max_i \|b^i\|_\infty \sqrt{d} \|\nabla u\|_{L^2(\Omega)} \|\Delta u\|_{L^2(\Omega)} \\ &\quad - \|\theta\|_\infty \|c^1\|_\infty \|u\|_{L^2(\Omega)} \|\Delta u\|_{L^2(\Omega)} \\ &\geq \|\Delta u\|_{L^2(\Omega)}^2 - \frac{\sqrt{1-\epsilon}}{A} \|\Delta u\|_{L^2(\Omega)}^2 - C_m (\|\nabla u\|_{L^2(\Omega)} \|\Delta u\|_{L^2(\Omega)} + \|u\|_{L^2(\Omega)} \|\Delta u\|_{L^2(\Omega)}) \end{aligned}$$

where  $C_m = \max\{\|\theta\|_\infty \max_i \|b^i\|_\infty \sqrt{d}, \|\theta\|_\infty \|c^1\|_\infty\}$ . By Poincaré inequality, we have  $\|u\|_{L^2(\Omega)} \leq C \|\nabla u\|_{L^2(\Omega)} \leq C^2 \|\Delta u\|_{L^2(\Omega)}$  for some constant  $C$ . Using Theorem 4, it is followed that

$$\begin{aligned}
0 &\geq \|\Delta u\|_{L^2(\Omega)} - \frac{\sqrt{1-\epsilon}}{A} \|\Delta u\|_{L^2(\Omega)} - C_m (\|\nabla u\|_{L^2(\Omega)} + \|u\|_{L^2(\Omega)}) \\
&\geq \|\Delta u\|_{L^2(\Omega)} - \frac{\sqrt{1-\epsilon}}{A} \|\Delta u\|_{L^2(\Omega)} - C_m (C + C^2) \|u\|_{H^2(\Omega)} \\
&\geq \|\Delta u\|_{L^2(\Omega)} - \frac{\sqrt{1-\epsilon}}{A} \|\Delta u\|_{L^2(\Omega)} - \frac{C_m (C + C^2)}{A} \|\Delta u\|_{L^2(\Omega)} \\
&= \|\Delta u\|_{L^2(\Omega)} \left(1 - \frac{\sqrt{1-\epsilon}}{A} - \frac{C_m (C + C^2)}{A}\right).
\end{aligned}$$

If the term  $(1 - \frac{\sqrt{1-\epsilon}}{A} - \frac{C_m (C + C^2)}{A})$  is positive, then we can conclude that  $\Delta u = 0$ . Since  $\Delta u = 0$  and  $u = 0$  on  $\partial\Omega$ ,  $\|u\|_L = 0$  and then  $u = 0$ . Similar to the proof of other norms  $\|\cdot\|_L$  and  $\|\cdot\|_{\mathcal{L}}$ , it is easy to prove that  $\|u + v\|_{\mathcal{L}_1} \leq \|u\|_{\mathcal{L}_1} + \|v\|_{\mathcal{L}_1}$  and  $\|au\|_{\mathcal{L}_1} = |a| \|u\|_{\mathcal{L}_1}$ . The detail is omitted.

**Theorem 10** *Assume that  $(1 - \frac{\sqrt{1-\epsilon}}{A} - \frac{C_m (C + C^2)}{A}) > 0$ . There exist two positive constants  $A_2$  and  $B_2$  such that*

$$A_2 \|u\|_{H^2(\Omega)} \leq \|u\|_{\mathcal{L}} \leq B_2 \|u\|_{H^2(\Omega)}, \quad \forall u \in H^2(\Omega) \cap H_0^1(\Omega). \quad (34)$$

*Proof.* The proof is similar to before. We leave it to the interested reader.  $\square$

Therefore, we can get the following theorem for the general elliptic PDE:

**Theorem 11** *Suppose  $\Omega \subset \mathbb{R}^d$  be a bounded domain and the closure of  $\Omega$  is of uniformly positive reach  $r_\Omega > 0$ . Assume that  $a^{ij}, b^i, c^1 \in L^\infty(\Omega)$  satisfy (25), (26), (27) and  $(1 - \frac{\sqrt{1-\epsilon}}{A} - \frac{C_m (C + C^2)}{A}) > 0$ . Suppose that  $u \in H^3(\Omega)$  and  $u - u_s = 0$  on  $\partial\Omega$ . For the solution  $u$  of equation (2) and the corresponding minimizer  $u_s$ , we have the following inequality*

$$\|u - u_s\|_{L^2(\Omega)} \leq C \epsilon_1$$

for a positive constant  $C$  depending on  $\Omega$  and a constant  $A_2$  in Theorem 10.

Finally we show that the convergence of  $\|u - u_s\|_{L^2(\Omega)}$  and  $\|\nabla(u - u_s)\|_{L^2(\Omega)}$  can be better

**Theorem 12** *Suppose that the bounded domain  $\Omega$  has an uniformly positive reach. Suppose  $f$  and  $g$  are continuous over bounded domain  $\Omega \subseteq \mathbb{R}^d$  for  $d = 2, 3$ . Suppose that  $u \in H^3(\Omega)$ . If  $u - u_s|_{\partial\Omega} = 0$ , we further have the following inequality*

$$\|u - u_s\|_{L^2(\Omega)} \leq C |\Delta|^2 \epsilon_1 \quad \text{and} \quad \|\nabla(u - u_s)\|_{L^2(\Omega)} \leq C |\Delta| \epsilon_1$$

for a positive constant  $C = 1/A_2$ , where  $A_2$  is one of the constants in Theorem 4 and  $|\Delta|$  is the size of the underlying triangulation  $\Delta$ .

*Proof.* The proof is similar to Theorem 6. We leave the detail to the interested reader.  $\square$

## 5 Implementation of the Spline based Collocation Method

Before we present our computational results for Poisson equation and general second order elliptic equations, let us first explain the implementation of our spline based collocation method. We divide the implementation into two parts. The first part of the implementation is to construct the collocation matrices  $K$  associated with the Poisson equation and  $\mathcal{K}$  associated with the general second order PDE in the non-divergence form over triangulation/tetrahedralization, the degree  $D$  of spline functions and the smoothness  $r \geq 1$  as well as the domain points  $\mathcal{D}_{D',\Delta}$  associated with the triangulation/tetrahedralization. This part also generates the smoothness matrix  $H, H_0$ . More precisely, for the Poisson equation, we construct collocation matrices

$$MxxV := [(B_{ijk}^t(\mathbf{x})_{xx}|_{\mathbf{x}=\xi_\ell}, \xi_\ell \in \mathcal{D}_{D',\Delta}] \text{ and } MyyV := [(B_{ijk}^t(\mathbf{x})_{yy}|_{\mathbf{x}=\xi_\ell}, \xi_\ell \in \mathcal{D}_{D',\Delta}]. \quad (35)$$

In fact we choose many other points which are in addition to the domain points to build these  $MxxV$  and  $MyyV$  to get better accuracy. For example, we choose  $D' = D + 3$  to generate domain points. Then  $K = MxxV + MyyV$  is a size of  $M \times m$  for the Poisson equation, where  $m = \dim(S_D^{-1}(\Delta))$  and  $M = \dim(S_{D'}^{-1}(\Delta))$ . After generating matrices, we save our matrices which will be used later for solution of the Poisson equation for various right-hand side functions and various boundary conditions.

For the general elliptic equations, we also generate all the related matrices  $MxxV, MxyV, MyyV, MxV, MyV, \dots$  similar to the matrices  $MxxV, MyyV$  for the Poisson equation. Then we generate the collocation matrix  $\mathcal{K}$  associated with the PDE coefficients at the same domain points from all the related matrices  $MxxV, MxyV, MyyV, MxV, MyV, \dots$  which are just generated before. This part is the most time consuming step. See Tables 1 and 2 for the 2D and 3D settings.

The second part, Part 2 is to construct the right-hand side vector  $\mathbf{f}$  for each given PDE problem and the matrix  $B$  and vector  $G$  associated with the boundary condition and use Algorithm 1 to solve the minimization problem (16) and (29). We shall use the four different domains in 2D shown in Fig. 1 and four different domains in 3D shown in Fig. 2 to test the performance of our collocation method. In addition, the spline based collocation method has been tested over many more domains of interest. In particular, many domains which are not positive reach are used for test and these numerical results can be found in [14].

In our computational experiments, we use a cluster computer at University of Georgia to generate the related collocation matrices for various degree of splines and domain points as described in the part I. We use multiple CPUs in the computer so that multiple operations can be done simultaneously. For the 2D case, we use 8 processors on a parallel computer, which has AMD Ryzen 7 4800H with Radeon Graphics 2.90 GHz for Part 1 and Part 2. And we also use a high memory (512GB) node from the Sapelo 2 cluster at University of Georgia, which has four AMD Opteron 6344 2.6 GHz processors. Using 48 processors on the UGA cluster, we can generate our necessary matrices and the computational times for Part 1 are listed in Table 1. For 3D case, we use 48 processors for Part 1 and 12 processors for Part 2 to do the computation. Tables 2 and 3 show the computational times for generating collocation matrices, where (P), (UGA P) indicates the time for the Poisson equation with 8 processors and 48 processors respectively and (G), (UGA G) for the general second order PDE using 2 processors and 48 processors, respectively.

Another issue of our computation is how to choose  $\alpha, \beta$ , and  $\gamma$  in our Algorithm 1. As



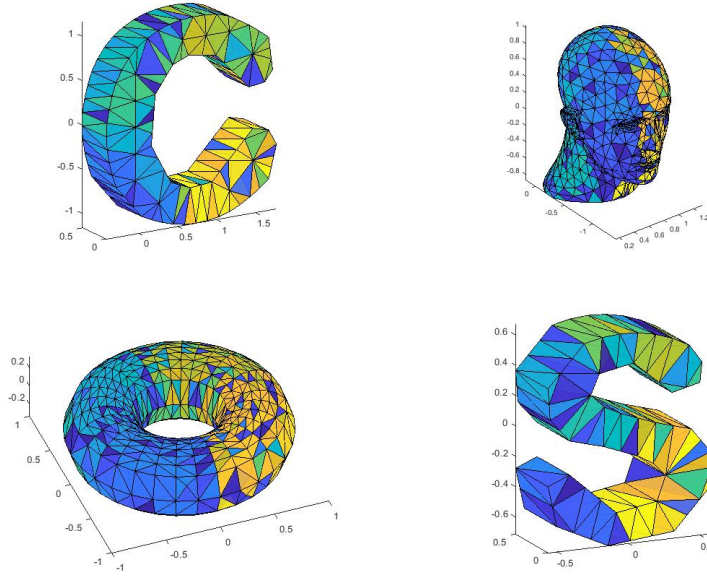


Figure 2: Several 3D domains used for Numerical Experiments

Domains	Number of vertices	Number of triangles	degree	Time (P)	Time (G)	Time (UGA P)	Time (UGA G)
Moon	325	531	8	4.04e+00	9.16e+00	9.66e+00	9.39e+00
Flower	297	494	8	2.50e+00	7.17e+00	4.35e+00	7.70e+00
Star	231	366	8	1.81e+00	5.03e+00	2.67e+00	6.31e+00
Circle	525	895	8	6.93e+00	1.85e+01	1.11e+01	1.78e+01

Table 1: Times in seconds for generating necessary matrices for each 2D domain in Figure 1.

there are many numerical solutions, we need to decide which one to choose. That is, if we are interested more in the accuracy of numerical solutions than the representation of the spline solutions, we use  $\alpha \geq 100$  while  $\beta = \gamma = 1$ . On the other hand, if we are interested more in the representation of spline solutions, we use  $\alpha = 1$  while  $\beta = \gamma \geq 10^5$  or  $\beta = 1$  and  $\gamma = 10^5$ . Let us present Table 4 to show these phenomena. The numerical results in Table 4 are based on spline functions of degree  $D = 8$  and smoothness  $r = 2$  over one of four domains in Figure 1 for all the testing functions listed in the next subsection. The rooted mean square(RMS) of vectors  $B\mathbf{c} - G$ ,  $H_0\mathbf{c}$ ,  $H_r\mathbf{c}$ ,  $u - u_s$  and  $\nabla(u - u_s)$  is computed based on those  $1001^2$  equally-spaced points over the bounding box of the domain which fall into the domain. From Table 4, we can see that when  $\alpha = 100$  while  $\beta = \gamma = 1$ , the RMS of the error vectors  $u - u_s$  and  $\nabla(u - u_s)$  is much

Domains	Number of vertices	Number of tetrahedron	Degree of splines	Time (UGA P)	Time (UGA G)
Letter C	190	431	9	5.50e+01	9.64e+01
Letter S	115	171	9	1.11e+01	2.91e+01
Torus	773	2911	9	1.55e+03	1.82e+03
Human head	913	1588	9	4.94e+02	6.52e+02

Table 2: Times in seconds for generating necessary matrices for each 3D domain in Figure 2.

Domain	Time (P)	Time (SG)	Time (NSG1)	Time (NSG2)
Letter C	3.7090e+00	6.0376e+00	6.0771e+00	5.8789e+00
Letter S	2.0961e+00	2.4158e+00	2.3350e+00	2.4420e+00
Torus	4.0213e+02	5.9574e+02	2.8542e+02	1.8183e+02
Human head	2.7215e+01	4.8097e+01	4.8966e+01	4.8966e+01

Table 3: Times in seconds for finding solutions of 3D Poisson equation(P), general second order elliptic equation with smooth PDE coefficients (SG) or with non-smooth PDE coefficients (NSG1, NSG2) for each domain in Figure 2.

smaller than the case when  $\alpha = \beta = 1$  and  $\gamma = 10^5$ . In the later case, the spline solution with RMS of  $H_0\mathbf{c}$  is within the machine epsilon and thus is a continuous function, but the accuracy is compromised. Therefore, in the remaining part of the paper, we simply use the setting  $\alpha = 100$  while  $\beta = \gamma = 1$  to show our computational results.

	Star with 2 holes( $\alpha = 10^2, \beta = \gamma = 1$ )					Star with 2 holes( $\alpha = \beta = \gamma = 1$ )				
	$B\mathbf{c} - G$	$H_0\mathbf{c}$	$H\mathbf{c}$	$u - u_s$	$\nabla(u - u_s)$	$B\mathbf{c} - G$	$H_0\mathbf{c}$	$H_r\mathbf{c}$	$u - u_s$	$\nabla(u - u_s)$
$u^{s1}$	1.83e-14	1.09e-13	1.25e-13	1.54e-12	5.73e-11	4.68e-13	1.15e-13	1.30e-13	1.67e-12	6.57e-11
$u^{s2}$	1.34e-13	1.95e-13	6.28e-13	3.37e-12	7.93e-11	1.24e-12	1.88e-13	2.78e-13	2.46e-12	9.77e-11
$u^{s3}$	1.01e-14	6.48e-14	7.52e-14	7.08e-13	3.36e-11	3.14e-13	9.37e-14	1.05e-13	1.48e-12	5.66e-11
$u^{s4}$	1.19e-13	3.10e-13	6.76e-13	1.47e-12	8.22e-11	1.45e-12	1.77e-13	2.68e-13	1.45e-12	8.41e-11
$u^{s5}$	1.06e-11	5.79e-11	1.56e-10	4.78e-10	1.52e-08	2.32e-10	5.14e-11	1.34e-10	3.02e-10	1.36e-08
$u^{s6}$	1.83e-15	1.14e-14	2.33e-14	1.25e-13	4.92e-12	5.32e-14	1.31e-14	2.15e-14	2.97e-13	7.23e-12
$u^{s7}$	1.17e-15	9.25e-15	1.03e-14	2.19e-13	5.42e-12	5.43e-14	1.04e-14	1.16e-14	2.81e-13	6.69e-12
$u^{s8}$	7.87e-06	2.55e-05	7.61e-05	1.06e-04	4.06e-03	1.49e-04	1.73e-05	3.65e-05	4.84e-05	3.36e-03
$u^{ns1}$	1.32e-08	7.47e-07	2.27e-06	2.59e-06	3.89e-04	3.87e-07	7.47e-07	2.26e-06	2.62e-06	3.89e-04
$u^{ns2}$	2.83e-06	1.06e-05	2.25e-05	4.69e-05	1.48e-03	4.99e-05	4.12e-06	7.02e-06	2.75e-05	9.76e-04
	Star with 2 holes( $\alpha = 1, \beta = \gamma = 10^5$ )					Star with 2 holes( $\alpha = \beta = 1, \gamma = 10^5$ )				
	$B\mathbf{c} - G$	$H_0\mathbf{c}$	$H_r\mathbf{c}$	$u - u_s$	$\nabla(u - u_s)$	$B\mathbf{c} - G$	$H_0\mathbf{c}$	$H_r\mathbf{c}$	$u - u_s$	$\nabla(u - u_s)$
$u^{s1}$	8.38e-10	1.97e-14	3.47e-14	9.82e-08	1.34e-06	7.21e-11	1.60e-15	6.45e-11	1.07e-08	1.47e-07
$u^{s2}$	1.43e-09	4.02e-14	6.53e-14	1.91e-07	2.60e-06	1.01e-10	3.26e-15	1.35e-10	1.76e-08	2.83e-07
$u^{s3}$	6.02e-10	1.47e-14	2.31e-14	7.49e-08	1.02e-06	5.15e-11	1.52e-15	6.25e-11	5.53e-09	1.00e-07
$u^{s4}$	1.20e-09	3.17e-14	5.34e-14	9.74e-08	1.42e-06	7.35e-11	2.30e-15	9.48e-11	7.78e-09	1.47e-07
$u^{s5}$	4.27e-10	1.33e-14	2.35e-14	2.34e-08	3.47e-07	2.44e-10	2.06e-15	1.37e-10	4.55e-09	7.04e-08
$u^{s6}$	2.09e-10	3.76e-15	6.46e-15	3.66e-09	6.80e-08	9.78e-12	2.19e-16	8.69e-12	9.66e-10	1.53e-08
$u^{s7}$	1.07e-10	3.13e-15	5.26e-15	7.50e-09	1.11e-07	7.15e-12	2.70e-16	1.12e-11	6.15e-10	1.18e-08
$u^{s8}$	2.12e-04	3.46e-09	6.32e-09	5.79e-05	4.44e-03	1.61e-04	7.13e-10	3.50e-05	4.86e-05	3.43e-03
$u^{ns1}$	8.62e-07	9.43e-11	1.77e-10	4.78e-06	4.56e-04	3.97e-07	2.80e-11	2.22e-06	3.44e-06	3.94e-04
$u^{ns2}$	6.89e-05	2.82e-10	4.92e-10	2.81e-05	1.08e-03	5.25e-05	1.50e-10	7.03e-06	2.89e-05	9.71e-04

Table 4: The RMS of vectors  $B\mathbf{c} - G$ ,  $H_0\mathbf{c}$ ,  $H_r\mathbf{c}$ , and the errors  $u - u_s$  and  $\nabla(u - u_s)$  for various  $\alpha, \beta$ , and  $\gamma$ .

## 6 Numerical results for the Poisson Equation

We shall present computational results for 2D Poisson equation and 3D Poisson equations separately in the following two subsections. In each section, we first present the computational results from the spline based collocation method to demonstrate the accuracy the method can achieve. Then we present a comparison of our collocation method with the numerical method proposed in [1] which uses multivariate splines to find the weak solution like finite element method. For convenience, we shall call our spline based collocation method the LL method and the numerical method in [1] the AWL method.

## 6.1 Numerical examples for 2D Poisson equations

We have used various triangulations over various bounded domains to experiment the performance of our Algorithm 1 in [14] and tested many solutions to the Poisson equation to see the accuracy that the LL method can do. For convenience, we shall only present a few of the computational results based on the domains in Figure 1. The following is a list of 10 testing functions (8 smooth solutions and 2 not very smooth)

$$\begin{aligned}
 u^{s1} &= e^{\frac{(x^2+y^2)}{2}}, \\
 u^{s2} &= \cos(xy) + \cos(\pi(x^2 + y^2)), \\
 u^{s3} &= \frac{1}{1 + x^2 + y^2}, \\
 u^{s4} &= \sin(\pi(x^2 + y^2)) + 1, \\
 u^{s5} &= \sin(3\pi x) \sin(3\pi y), \\
 u^{s6} &= \arctan(x^2 - y^2), \\
 u^{s7} &= -\cos(x) \cos(y) e^{-(x-\pi)^2 - (y-\pi)^2}, \\
 u^{s8} &= \tanh(20y - 20x^2) - \tanh(20x - 20y^2), \\
 u^{ns1} &= |x^2 + y^2|^{0.8} \text{ and} \\
 u^{ns2} &= (xe^{1-|x|} - x)(ye^{1-|y|} - y).
 \end{aligned}$$

Note that the test function in  $u^{s8}$  is notoriously difficult to solve. One has to use a good adaptive triangulation method (cf. [8]). The rooted mean square (RMS) of  $u - u_s$  and  $\nabla(u - u_s)$  of approximate spline solution  $u_s$  against the exact solution  $u$  are given in Table 5. These errors are computed based on  $1001 \times 1001$  equally-spaced points fell inside the different domains in Figure 1. We chose collocation points to create  $M \times m$  matrix  $K$ , where  $m$  is the number of Bernstein basis functions (the dimension of spline space  $S_D^{-1}(\Delta)$ ) and Algorithm 1 is used to find the numerical solutions.

Solution	Moon		Flower with a hole		Star with 2 holes		Circle with 3 holes	
	$u - u_s$	$\nabla(u - u_s)$	$u - u_s$	$\nabla(u - u_s)$	$u - u_s$	$\nabla(u - u_s)$	$u - u_s$	$\nabla(u - u_s)$
$u^{s1}$	6.95e-11	4.15e-10	1.23e-11	1.54e-10	1.67e-12	6.57e-11	1.63e-11	1.68e-10
$u^{s2}$	3.53e-10	4.81e-09	1.83e-11	8.79e-10	2.46e-12	9.77e-11	2.65e-11	2.55e-10
$u^{s3}$	2.58e-11	1.81e-10	6.96e-12	9.48e-11	1.48e-12	5.66e-11	8.03e-12	8.73e-11
$u^{s4}$	2.53e-10	3.57e-09	2.19e-11	6.80e-10	1.45e-12	8.41e-11	1.92e-11	2.00e-10
$u^{s5}$	6.16e-08	1.44e-06	7.73e-09	2.57e-07	3.02e-10	1.36e-08	5.33e-10	1.87e-08
$u^{s6}$	1.75e-11	2.86e-10	3.23e-12	8.71e-11	2.97e-13	7.23e-12	7.51e-12	7.85e-11
$u^{s7}$	3.07e-12	2.27e-11	1.15e-12	1.51e-11	2.81e-13	6.69e-12	1.10e-12	1.28e-11
$u^{s8}$	1.06e-03	9.32e-02	8.65e-04	8.38e-02	4.84e-05	3.36e-03	5.21e-04	2.09e-02
$u^{ns1}$	7.31e-10	3.68e-08	5.18e-06	4.94e-04	2.62e-06	3.89e-04	1.80e-05	3.22e-04
$u^{ns2}$	3.16e-04	2.61e-03	7.39e-05	1.51e-03	2.75e-05	9.76e-04	1.91e-05	6.25e-04

Table 5: The RMS of errors  $u - u_s$  and  $\nabla u - \nabla u_s$  for Poisson equations for four domains showed in Figure 1 when  $r = 2$  and  $D = 8$ .

From Table 5, we can see that the performance of our method is excellent. Next let us compare with the numerical method in [1] for the same degree, the same smoothness, and the same triangulation. The comparison results are shown in Table 6. One can see that both methods perform very well. Our method can achieve a better accuracy due to the reason the more number of collocation points is used than the dimension of spline space  $S_D^{-1}(\Delta)$ .

Sol'n	Moon		Flower with a hole		Star with 2 holes		Circle with 3 holes	
	AWL	LL	AWL	LL	AWL	LL	AWL	LL
$u^{s1}$	1.51e-07	6.95e-11	1.14e-07	1.23e-11	2.08e-07	1.67e-12	5.22e-08	1.63e-11
$u^{s2}$	1.33e-07	3.53e-10	3.79e-07	1.83e-11	8.93e-07	2.46e-12	2.35e-08	2.65e-11
$u^{s3}$	4.94e-08	2.58e-11	8.07e-08	6.96e-12	1.44e-07	1.48e-12	1.62e-08	8.03e-12
$u^{s4}$	5.77e-07	2.53e-10	3.89e-07	2.19e-11	4.51e-07	1.45e-12	2.02e-07	1.92e-11
$u^{s5}$	1.58e-06	6.16e-08	1.43e-06	7.73e-09	1.67e-06	3.02e-10	2.65e-07	5.33e-10
$u^{s6}$	5.00e-07	1.75e-11	1.44e-07	3.23e-12	4.03e-07	2.97e-13	9.47e-08	7.51e-12
$u^{s7}$	1.99e-08	3.07e-12	2.20e-08	1.15e-12	3.30e-08	2.81e-13	4.97e-09	1.10e-12
$u^{s8}$	1.31e-03	1.06e-03	1.19e-03	8.65e-04	1.49e-04	4.84e-05	7.96e-04	5.21e-04
$u^{ns1}$	1.50e-07	7.31e-10	2.39e-04	5.18e-06	2.26e-05	2.62e-06	1.43e-05	1.80e-05
$u^{ns2}$	1.38e-03	3.16e-04	4.55e-04	7.39e-05	9.87e-05	2.75e-05	8.57e-05	1.91e-05

Table 6: RMSE of spline solutions for the Poisson equation over the four domains in Figure 1 when  $r = 2$  and  $D = 8$  for both the AWL method and the LL method.

Domain	Number of vertices	Number of triangles	Average time for AWL method	Average time for LL method (part 2)
Moon	325	531	9.61e-01	6.28e-01
Flower with a hole	297	494	8.05e-01	5.39e-01
Star with 2 holes	231	366	5.53e-01	3.97e-01
Circle with 3 holes	525	895	1.44e+00	9.74e-01

Table 7: The number of vertices, triangles and the averaged time for solving the 2D Poisson equation for each domain in Figure 1.

Finally, we summarize the computational times for both methods in Table 7. One can see the LL method can be more efficient if the collocation matrices are already generated. The LL method can be useful for time dependent PDE such as the heat equation. We only need to generate the collocation matrix once and use it repeatedly for many time step iterations.

## 6.2 Numerical results for the 3D Poisson equation

We have used our collocation method to solve the 3D Poisson equation and the tested 10 smooth and non-smooth solution over various domains. For convenience, we only show a few computational results to demonstrate that our collocation method works very well. More detail can be found in [14]. Our testing smooth solutions are as follows:

$$\begin{aligned}
u^{3ds1} &= \sin(2x + 2y) \tanh\left(\frac{xz}{2}\right) \\
u^{3ds2} &= e^{\frac{x^2+y^2+z^2}{2}} \\
u^{3ds3} &= \cos(xyz) + \cos(\pi(x^2 + y^2 + z^2)) \\
u^{3ds4} &= \frac{1}{1 + x^2 + y^2 + z^2} \\
u^{3ds5} &= \sin(\pi(x^2 + y^2 + z^2)) + 1 \\
u^{3ds6} &= 10e^{-x^2-y^2-z^2} \\
u^{3ds7} &= \sin(2\pi x) \sin(2\pi y) \sin(2\pi z) \\
u^{3ds8} &= z \tanh((- \sin(x) + y^2)) \\
u^{3dns1} &= |x^2 + y^2 + z^2|^{0.8} \\
u^{3dns2} &= (xe^{1-|x|} - x)(ye^{1-|y|} - y)(ze^{1-|z|} - z).
\end{aligned}$$

The rooted mean squared errors of approximate spline solutions against the exact solution

Solution	Letter C		Letter S		Torus		Human head	
	$u - u_s$	$\nabla(u - u_s)$	$u - u_s$	$\nabla(u - u_s)$	$u - u_s$	$\nabla(u - u_s)$	$u - u_s$	$\nabla(u - u_s)$
$u^{3ds1}$	2.31e-11	2.52e-10	3.01e-12	4.58e-11	7.87e-11	1.40e-09	4.12e-10	5.02e-09
$u^{3ds2}$	5.47e-10	4.86e-09	7.53e-12	7.31e-11	4.52e-09	3.24e-08	1.66e-08	1.29e-07
$u^{3ds3}$	5.49e-07	8.40e-06	8.87e-08	7.80e-07	3.32e-09	3.21e-08	9.96e-06	1.65e-04
$u^{3ds4}$	4.83e-09	5.09e-08	4.29e-09	3.85e-08	2.16e-09	1.61e-08	1.13e-08	2.21e-07
$u^{3ds5}$	6.49e-07	1.67e-05	1.17e-07	9.47e-07	7.07e-09	5.78e-08	3.62e-06	5.88e-05
$u^{3ds6}$	3.52e-09	3.99e-08	8.39e-10	6.53e-09	2.03e-08	1.72e-07	6.69e-08	6.90e-07
$u^{3ds7}$	9.14e-06	8.63e-05	3.20e-06	2.44e-05	1.40e-07	4.75e-06	4.31e-05	8.24e-04
$u^{3ds8}$	2.05e-08	2.79e-07	3.30e-09	3.35e-08	1.76e-10	2.98e-09	1.90e-08	3.94e-07
$u^{3dns1}$	8.80e-06	4.66e-04	3.17e-05	1.14e-03	2.23e-09	1.80e-08	8.28e-06	2.18e-03
$u^{3dns2}$	8.39e-05	1.20e-03	4.30e-05	4.65e-04	1.20e-04	2.49e-03	8.90e-04	5.18e-02

Table 8: RMS of error vectors  $u - u_s$  and  $\nabla u - \nabla u_s$  for the 3D Poisson equation over the four domains in Figure 2 based on trivariate spline functions of smoothness  $r = 1$  and degree  $D = 9$

Solution	Torus				Human head			
	AWL		LL		AWL		LL	
	$u - u_s$	$\nabla(u - u_s)$	$u - u_s$	$\nabla(u - u_s)$	$u - u_s$	$\nabla(u - u_s)$	$u - u_s$	$\nabla(u - u_s)$
$u^{3ds1}$	3.55e-09	5.74e-07	1.79e-10	2.04e-09	2.83e-09	7.56e-07	5.83e-12	6.45e-11
$u^{3ds2}$	2.92e-08	1.98e-06	1.14e-08	8.50e-08	5.21e-07	2.72e-06	3.45e-10	2.95e-09
$u^{3ds3}$	1.07e-07	8.90e-06	5.34e-09	3.31e-08	6.44e-08	1.21e-05	7.26e-10	8.21e-09
$u^{3ds4}$	1.88e-08	1.46e-06	3.57e-09	2.29e-08	1.83e-08	2.72e-06	2.68e-10	2.76e-09
$u^{3ds5}$	8.25e-08	5.50e-06	1.33e-08	8.95e-08	6.09e-08	8.43e-06	9.75e-10	5.78e-09
$u^{3ds6}$	2.50e-07	1.80e-05	3.39e-08	1.90e-07	1.31e-07	1.35e-05	2.35e-09	2.47e-08
$u^{3ds7}$	8.07e-08	5.83e-06	1.01e-07	2.34e-06	1.88e-08	2.72e-06	4.19e-08	5.21e-07
$u^{3ds8}$	8.16e-09	7.24e-07	6.42e-10	4.32e-09	8.16e-09	3.41e-07	2.69e-11	1.66e-10
$u^{3dns1}$	3.92e-08	2.67e-06	5.07e-09	3.22e-08	3.63e-08	2.67e-06	3.82e-06	6.23e-04
$u^{3dns2}$	6.30e-04	2.29e-03	1.09e-04	1.58e-03	3.42e-04	2.49e-03	2.30e-04	4.84e-03

Table 9: The RMSE of spline solutions for the 3D Poisson equation over the two domains in Figure 2 based on trivariate spline functions of smoothness  $r = 1$  and degree  $D = 9$  for the AWL method and LL method.

are computed based on  $501 \times 501 \times 501$  equally-spaced points over the different domains shown Figure 2.

We choose collocation points to create  $M \times m$  matrix  $K$ , where  $m$  is the dimension of spline space  $S_D^{-1}(\Delta)$  and apply Algorithm 1 to find the numerical solutions. We tested 10 functions over the domains in Figure 2. Their root mean square errors are presented in Table 8. We also compare the AWL method with LL method for the numerical solution of the 3D Poisson equation. See numerical results in Table 9 which show that the LL method is more accurate than the AWL method when the solutions are smooth and is similar to the AWL method when the solutions are not very smooth.

## 7 Numerical Results for General Second Order Elliptic PDE

We shall present computational results for 2D and 3D general second order PDEs separately in the following two subsections. In each section, we first present the computational results from the spline based collocation method to demonstrate the accuracy the method can achieve. Then we present a comparison of our collocation method with the numerical method based on [11]. For convenience, we shall call our spline based collocation method the LL method and the numerical method in [11] the LW method.

## 7.1 Numerical examples for 2D general second order equations

We have used the same triangulations over various bounded domains as shown in Figure 1 and tested the same solutions which we used for the Poisson equation for the general second order equation to see the accuracy that the LL method can have. The root mean squared error (RMSE)  $u - u_s$  and  $\nabla u - \nabla u_s$  of approximate spline solutions  $u_s, \nabla u_s$  against the exact solutions  $u, \nabla u$  are given in Tables in this section. The RMSE are computed based on  $1001 \times 1001$  equally-spaced points fell inside the different domains in Figure 1. We chose additional collocation points to create  $M \times m$  matrix  $\mathcal{K}$ , where  $m, M$  are the dimension of spline space  $S_D^{-1}(\Delta)$  and  $S_{D'}^{-1}(\Delta)$ , respectively.

### 7.1.1 2D general second order equations with smooth coefficients

**Example 1** We first tested our computational method to solve the 2nd order elliptic equation with smooth PDE coefficients:  $a_{11} = x^2 + y^2, a_{12} = \cos(xy), a_{21} = e^{xy}, a_{22} = x^3 + y^2 - \sin(x^2 + y^2), b_1 = 3 \cos(x)y^2, b_2 = e^{-x^2 - y^2}, c = 0$ . Our testing functions are 2 non-smooth solutions  $u^{ns1}, u^{ns2}$ , and 8 smooth solutions  $u^{s1} - u^{s8}$  given in the previous section. The RMS of error vectors  $u - u_s$  and  $\nabla(u - u_s)$  over the four domains in Figure 1 is presented in Table 10. The numerical results show that the LL method works very well.

Solution	Moon		Flower with a hole		Star with 2 holes		Circle with 3 holes	
	$u - u_s$	$\nabla(u - u_s)$	$u - u_s$	$\nabla(u - u_s)$	$u - u_s$	$\nabla(u - u_s)$	$u - u_s$	$\nabla(u - u_s)$
$u^{s1}$	3.11e-10	6.25e-09	1.63e-10	5.62e-09	4.96e-11	1.93e-09	4.05e-10	1.06e-08
$u^{s2}$	7.86e-10	1.51e-08	6.95e-10	2.98e-08	1.33e-10	4.04e-09	3.27e-10	1.18e-08
$u^{s3}$	2.90e-10	4.12e-09	1.72e-10	4.77e-09	4.07e-11	1.60e-09	1.78e-10	6.25e-09
$u^{s4}$	4.79e-10	1.51e-08	4.38e-10	1.59e-08	5.33e-11	2.41e-09	5.05e-10	1.26e-08
$u^{s5}$	5.35e-08	3.40e-06	5.90e-08	2.58e-06	8.84e-10	6.81e-08	3.04e-09	1.93e-07
$u^{s6}$	1.24e-10	2.52e-09	4.19e-11	1.83e-09	1.11e-11	3.56e-10	1.29e-10	2.44e-09
$u^{s7}$	2.65e-11	4.32e-10	3.02e-11	1.40e-09	7.06e-12	3.07e-10	5.81e-11	1.23e-09
$u^{s8}$	9.04e-03	2.61e-01	9.81e-03	3.63e-01	2.50e-04	1.35e-02	2.28e-03	1.29e-01
$u^{ns1}$	8.26e-10	6.54e-08	4.62e-06	6.85e-04	1.69e-06	4.87e-04	5.78e-05	6.17e-03
$u^{ns2}$	2.01e-04	3.24e-03	2.97e-04	6.88e-03	1.27e-04	5.80e-03	7.33e-05	2.84e-03

Table 10: RMSE of spline solutions for general second order elliptic equations with smooth coefficients over the four domains in Figure 1 when  $r = 2$  and  $D = 8$ .

### 7.1.2 2D general second order equations with non-smooth coefficients

**Example 2** In [18], the researchers experimented their numerical methods for the second order PDE as follows:

$$\sum_{i,j=1}^2 (1 + \delta_{ij}) \frac{x_i}{|x_i|} \frac{x_j}{|x_j|} u_{x_i x_j} = f \quad \text{in } \Omega, \quad u = 0 \quad \text{on } \partial\Omega,$$

where  $\Omega = (-1, 1)^2$  and the solution  $u$  is  $u(x, y) = (xe^{1-|x|} - x)(ye^{1-|y|} - y)$  which is one of our testing functions. It is easy to see those coefficients satisfy the Cordes condition

$$\frac{\sum_{i,j=1}^d (a_{i,j})^2}{(\sum_{i=1}^d a_{ii})^2} = \frac{2^2 + 1 + 1 + 2^2}{(2 + 2)^2} = \frac{10}{16} \leq \frac{1}{2 - 1 + \epsilon}$$

Solution	Moon		Flower with a hole		Star with 2 holes		Circle with 3 holes	
	$u - u_s$	$\nabla(u - u_s)$	$u - u_s$	$\nabla(u - u_s)$	$u - u_s$	$\nabla(u - u_s)$	$u - u_s$	$\nabla(u - u_s)$
$u^{s1}$	1.36e-10	1.24e-09	8.79e-11	1.34e-09	2.85e-11	3.73e-09	1.03e-11	1.14e-10
$u^{s2}$	1.95e-10	2.59e-09	1.16e-10	2.15e-09	2.97e-11	2.02e-09	1.66e-11	1.73e-10
$u^{s3}$	5.20e-11	4.91e-10	5.21e-11	8.99e-10	1.52e-11	1.07e-09	5.20e-12	5.85e-11
$u^{s4}$	2.16e-10	2.46e-09	9.81e-11	1.83e-09	2.68e-11	2.06e-09	1.61e-11	1.82e-10
$u^{s5}$	6.26e-08	1.27e-06	1.33e-08	3.24e-07	5.04e-10	2.02e-08	7.58e-10	1.64e-08
$u^{s6}$	3.92e-11	4.46e-10	1.61e-11	2.63e-10	4.77e-12	2.07e-10	3.25e-12	3.81e-11
$u^{s7}$	3.43e-12	3.26e-11	1.26e-11	2.00e-10	2.81e-12	2.45e-10	1.22e-12	1.20e-11
$u^{s8}$	1.44e-03	9.95e-02	2.86e-03	1.20e-01	1.11e-04	4.07e-03	1.87e-04	1.67e-02
$u^{ns1}$	2.00e-09	5.73e-08	1.57e-04	3.88e-03	2.59e-04	4.30e-03	1.50e-05	5.31e-04
$u^{ns2}$	1.60e-03	1.62e-02	1.03e-03	1.73e-02	8.84e-04	1.61e-02	2.56e-04	4.03e-03

Table 11: RMSE  $u - u_s$  and  $\nabla u - \nabla u_s$  for the general elliptic equation with the non-smooth coefficients in Example 2 over the four domains in Figure 1 when  $r = 2$  and  $D = 8$ .

when  $\epsilon = \frac{3}{5}$ . This equation was also numerically experimented in [11] and [19].

Let us test our method on this 2nd order elliptic equation with non-smooth coefficients for the 2 non-smooth solutions  $u^{ns1}, u^{ns2}$ , and 8 smooth solutions  $u^{s1} - u^{s8}$  over the four domains used in the previous section. We use bivariate splines of degree  $D = 8$  and smoothness  $r = 2$  for the experiment. And the RMSE of the solutions for the four domains in Figure 1 are reported in Table 11. It is clear to see that our method works very well.

**Example 3** The second example in the paper [18] is another second order PDE:

$$\sum_{i,j=1}^2 (\delta_{ij} + \frac{x_i x_j}{|x|^2}) u_{x_i x_j} = f \text{ in } \Omega, \quad u = 0 \text{ on } \partial\Omega,$$

where  $\Omega = (-1, 1)^2$  and the solution  $u$  is  $u(x, y) = |x^2 + y^2|^{\frac{\alpha}{2}}$  which is on the list of our testing functions. Then those coefficients satisfy the Cordes condition when  $\epsilon = \frac{4}{5}$ .

Solution	Moon		Flower with a hole		Star with 2 holes		Circle with 3 holes	
	$u - u_s$	$\nabla(u - u_s)$	$u - u_s$	$\nabla(u - u_s)$	$u - u_s$	$\nabla(u - u_s)$	$u - u_s$	$\nabla(u - u_s)$
$u^{s1}$	2.20e-11	1.81e-10	2.26e-11	4.32e-10	1.04e-11	2.38e-09	6.64e-12	7.61e-11
$u^{s2}$	1.64e-10	2.67e-09	2.52e-11	1.03e-09	1.50e-11	2.49e-09	7.34e-12	1.04e-10
$u^{s3}$	1.41e-11	1.08e-10	1.72e-11	3.33e-10	9.64e-12	1.80e-09	4.03e-12	4.67e-11
$u^{s4}$	1.75e-10	2.14e-09	4.16e-11	9.44e-10	1.80e-11	3.92e-09	9.03e-12	1.22e-10
$u^{s5}$	3.71e-08	8.57e-07	6.13e-09	2.01e-07	3.78e-10	1.58e-08	5.95e-10	1.35e-08
$u^{s6}$	5.70e-12	2.31e-10	6.56e-12	1.31e-10	1.33e-12	2.73e-10	1.77e-12	2.38e-11
$u^{s7}$	1.42e-12	1.21e-11	3.23e-12	6.56e-11	1.24e-12	2.63e-10	4.61e-13	5.59e-12
$u^{s8}$	1.15e-03	8.63e-02	2.11e-03	8.77e-02	5.51e-05	3.41e-03	1.46e-04	1.61e-02
$u^{ns1}$	3.58e-10	4.08e-08	1.31e-04	3.45e-03	2.11e-04	4.12e-03	3.26e-05	1.01e-03
$u^{ns2}$	1.95e-04	1.97e-03	5.78e-05	1.35e-03	2.73e-05	9.06e-04	1.60e-05	5.25e-04

Table 12: The RMS of vectors  $u - u_s, \nabla u - \nabla u_s$  for general elliptic equations with non-smooth coefficients in Example 3 over the four domains when  $r = 2$  and  $D = 8$ .

Similar to Example 2, we use the LL method to solve the PDE above using the 10 testing functions based on bivariate splines of degree  $D = 8$  and smoothness  $r = 2$ . See Table 12 for the RMS of error vectors.

## 7.2 Comparison with Numerical Method in [11]

We first compare our LL method with the LW method in [11] when numerically solving three PDEs given in Examples 1, 2, and 3. The RMSEs from the two methods will be reported in Table 13. For simplicity, we only present the numerical results from the two computational methods over the Circle with 3 holes in Table 13. We get the similar results for other 2D domains in Figure 1. From Table 13, we see that the LL method produces more accurate results.

Method	PDE in Example 1		PDE in Example 2		PDE in Example 3	
	LW	LL	LW	LL	LW	LL
$u^{s1}$	2.01e-09	1.49e-10	2.15e-06	1.03e-11	7.47e-09	6.64e-12
$u^{s2}$	2.22e-08	4.31e-11	2.97e-05	1.66e-11	3.86e-08	7.34e-12
$u^{s3}$	1.70e-09	8.85e-11	4.96e-06	5.20e-12	2.97e-09	4.03e-12
$u^{s4}$	2.29e-08	2.12e-10	6.13e-05	1.61e-11	7.66e-08	9.03e-12
$u^{s5}$	8.24e-08	3.37e-09	4.19e-04	7.58e-10	1.20e-06	5.95e-10
$u^{s6}$	2.63e-09	3.72e-11	4.11e-06	3.25e-12	3.15e-09	1.77e-12
$u^{s7}$	3.06e-14	1.05e-11	2.10e-11	1.22e-12	2.66e-14	4.61e-13
$u^{s8}$	8.50e-04	2.26e-03	2.54e-03	1.87e-04	1.78e-04	1.46e-04
$u^{ns1}$	1.35e-05	4.83e-05	3.57e-05	1.50e-05	1.52e-05	3.26e-05
$u^{ns2}$	2.45e-04	4.56e-05	1.60e-04	2.56e-04	5.92e-05	1.60e-05

Table 13: The RMSE of spline solutions for general elliptic equations in Example 1, PDE with non-smooth coefficients in Example 2 and in Example 3 over the Circle with 3 holes when  $r = 2$  and  $D = 8$  for the LW method and the LL method, respectively.

Next Table 14 shows the averaged computational time for the LL method is shorter than the LW method.

Domain	Number of vertices	Number of triangles	Average time for LW method	Average time for Part 2 of LL method
Flower with a hole	297	494	1.3236e+02	3.521e-01
Circle with 3 holes	525	895	4.4387e+03	8.313e-01

Table 14: The number of vertices, triangles and the averaged time in seconds for solving 2D general second order equations over the four domains in Figure 1 by the LW and LL methods.

Combining the computational results in Table 14 and computational times in Table 13, we conclude that the LL method is more effective and efficient than the LW method.

## 8 The Rate of Convergence of the LL method

Finally, we discuss the rate of convergence of the LL method. First we consider the 2D general elliptic PDEs in Examples 1, 2, and 3 over  $[0, 1]^2$  using our 10 testing functions. See the rate of convergence in Table 15. In Example 5, we present the rate of convergence for 3D general elliptic PDE with smooth coefficients.

**Example 4** Table 15 presents the RMSEs ( $RMSE_1$ ,  $RMSE_2$ ) of spline solutions over two triangulations of  $[0, 1]^2$  as shown in Figure 3 with  $|\triangle| = \frac{\sqrt{2}}{2}$  and  $|\triangle| = \frac{\sqrt{2}}{4}$ , respectively. The rate of convergence is defined by  $RMSE_1/RMSE_2$ . We can see that the rate of convergence agrees with our theory for all smooth testing functions.



	PDE in Example 1			PDE in Example 2			Example 3		
	RMSE <sub>1</sub>	RMSE <sub>2</sub>	Rate	RMSE <sub>1</sub>	RMSE <sub>2</sub>	Rate	RMSE <sub>1</sub>	RMSE <sub>2</sub>	Rate
$u^{s1}$	2.25e-08	1.15e-10	1.96e+02	1.16e-08	3.73e-11	3.11e+02	1.09e-08	5.33e-11	2.05e+02
$u^{s2}$	3.74e-04	2.96e-06	1.26e+02	2.30e-04	1.00e-06	2.29e+02	1.70e-04	8.14e-07	2.09e+02
$u^{s3}$	1.50e-07	1.02e-09	1.46e+02	1.36e-07	8.16e-10	1.67e+02	1.44e-07	1.08e-09	1.33e+02
$u^{s4}$	2.42e-04	3.03e-06	7.96e+01	1.99e-04	1.07e-06	1.86e+02	1.55e-04	8.54e-07	1.81e+02
$u^{s5}$	1.25e-02	1.26e-04	9.88e+01	1.14e-02	2.74e-05	4.16e+02	7.20e-03	2.45e-05	2.94e+02
$u^{s6}$	2.02e-06	4.41e-08	4.59e+01	6.55e-07	8.46e-09	7.74e+01	7.34e-07	8.03e-09	9.14e+01
$u^{s7}$	2.60e-10	1.02e-12	2.55e+02	1.18e-10	3.32e-13	3.56e+02	1.31e-10	5.05e-13	2.59e+02
$u^{s8}$	5.60e-01	2.25e-01	2.49e+00	1.05e-01	7.00e-02	1.50e+00	1.07e-01	6.06e-02	1.76e+00
$u^{ns1}$	3.95e-05	7.47e-06	5.29e+00	2.13e-05	3.78e-06	5.63e+00	1.85e-05	5.03e-06	3.67e+00
$u^{ns2}$	9.36e-05	1.72e-05	5.43e+00	2.52e-09	8.62e-12	2.92e+02	9.57e-05	2.89e-05	3.31e+00

Table 15: The RMS of the error vector  $\mathcal{L}(u - u_s)$  for general elliptic equations with smooth coefficients in Example 1, general elliptic PDE with non-smooth coefficients in Example 2 and 3 over  $[0, 1]^2$  (RMSE<sub>1</sub> and RMSE<sub>2</sub> of spline solutions with  $|\Delta| = \frac{\sqrt{2}}{2}$  and  $|\Delta| = \frac{\sqrt{2}}{4}$ , respectively. Splines of smoothness  $r = 2$  and degree  $D = 8$  are used.

**Example 5** We tested a 2nd order elliptic equation (2) with smooth PDE coefficients  $a_{11} = x^2 + y^2$ ,  $a^{22} = \cos(xy - z)$ ,  $a^{33} = \exp(\frac{1}{x^2+y^2+z^2+1})$ ,  $a^{12} + a^{21} = x^2 - y^2 - z$ ,  $a^{23} + a^{32} = \cos(xy - z) \sin(x - y)$ ,  $a^{13} + a^{31} = \frac{1}{y^2+z^2+1}$ ,  $b_1 = 0$ ,  $b_2 = -1$ ,  $b_3 = \tan^{-1}(x^3 - y^2 + \cos(z))$ ,  $c = x + y + z$ , where  $a^{12} = a^{21}$ ,  $a^{32} = a^{23}$  and  $a^{13} = a^{31}$ . The testing functions are the 2 not very smooth solutions  $u^{ns1}$ ,  $u^{ns2}$ , and 8 smooth solutions  $u^{s1} - u^{s8}$  over the standard cube  $[0, 1]^3$  with two tetrahedrizations indicated in Figure 3. The RMS of the error vectors  $u - u_s$ ,  $\nabla(u - u_s)$ , and  $\mathcal{L}_1(u - u_s)$  based on  $501^3$  equally-spaced points over  $[0, 1]^3$  are reported in Table 16. We can see that the rate of convergence agrees with our theory for all smooth testing functions.

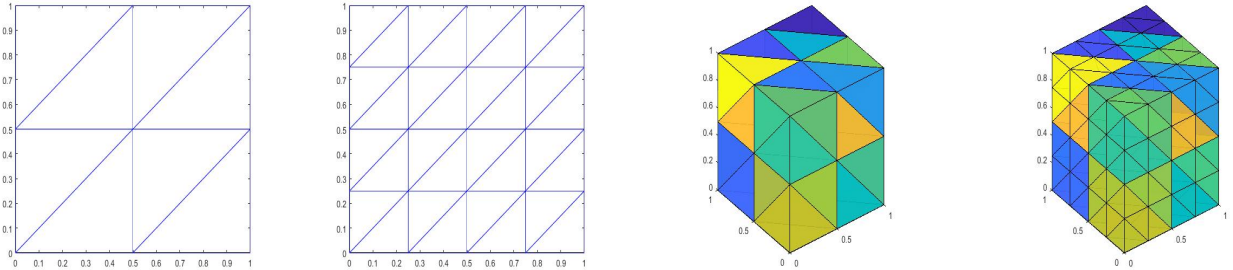


Figure 3: Several domains used for Numerical Experiments

## References

- [1] G. Awanou, M. -J. Lai, and P. Wenston, The multivariate spline method for scattered data fitting and numerical solution of partial differential equations. In Wavelets and splines: Athens 2005, pages 24–74. Nashboro Press, Brentwood, TN, 2006.
- [2] H. Brezis, Functional analysis, Sobolev spaces and partial differential equations, Springer, 2011.

Solution	$ \Delta  = \frac{\sqrt{2}}{2}$			$ \Delta  = \frac{\sqrt{2}}{4}$			rate		
	$u - u_s$	$\nabla(u - u_s)$	$\mathcal{L}_1(u - u_s)$	$u - u_s$	$\nabla(u - u_s)$	$\mathcal{L}_1(u - u_s)$	$u - u_s$	$\nabla(u - u_s)$	$\mathcal{L}_1(u - u_s)$
$u^{3ds1}$	5.94e-10	3.52e-08	8.25e-08	2.09e-11	3.71e-10	2.27e-09	2.84e+01	9.50e+01	3.64e+01
$u^{3ds2}$	1.16e-09	5.48e-08	4.17e-07	2.47e-10	7.37e-09	3.60e-08	4.68e+00	7.44e+00	1.16e+01
$u^{3ds3}$	2.03e-05	1.10e-03	8.61e-03	5.41e-08	3.96e-06	5.17e-05	3.75e+02	2.78e+02	1.66e+02
$u^{3ds4}$	2.91e-07	9.27e-06	4.39e-05	5.16e-10	3.18e-08	2.21e-07	5.63e+02	2.92e+02	1.99e+02
$u^{3ds5}$	1.17e-05	6.15e-04	4.74e-03	4.67e-08	4.02e-06	5.71e-05	2.50e+02	1.53e+02	8.30e+01
$u^{3ds6}$	7.74e-08	2.99e-06	1.36e-05	1.10e-09	3.78e-08	1.46e-07	7.03e+01	7.90e+01	9.35e+01
$u^{3ds7}$	9.82e-04	4.44e-02	3.45e-01	1.71e-06	1.30e-04	1.75e-03	5.74e+02	3.42e+02	1.97e+02
$u^{3ds8}$	6.23e-07	3.07e-05	1.94e-04	9.86e-10	1.05e-07	1.41e-06	6.32e+02	2.94e+02	1.38e+02
$u^{3dns1}$	1.10e-04	5.39e-03	4.72e-02	1.65e-05	1.62e-03	2.23e-02	6.69e+00	3.33e+00	2.11e+00
$u^{3dns2}$	4.60e-04	1.54e-02	6.71e-02	1.59e-04	7.43e-03	3.41e-02	2.89e+00	2.07e+00	1.97e+00

Table 16: RMS of the error vectors  $u - u_s$ ,  $\nabla u - \nabla u_s$ ,  $\mathcal{L}_1 u - \mathcal{L}_1 u_s$  for the general 2nd order elliptic equation in Example 5 over  $[0, 1]^3$  by using trivariate splines of degree  $D = 9$  and smoothness  $r = 1$ .

- [3] L. Evens, Partial Differential Equation. American Mathematical Society, Providence (1998)
- [4] F. Gao and M. -J. Lai, A new  $H^2$  regularity condition of the solution to Dirichlet problem of the Poisson equation and its applications, Acta Mathematica Sinica, vol. 36 (2020) pp. 21–39.
- [5] P. Grisvard, Elliptic Problems in Nonsmooth Domains, Pitman, 1985.
- [6] X.-L. Hu, D.-F. Han, and M.-J. Lai, Bivariate Splines of Various Degrees for Numerical Solution of Partial Differential Equations, SIAM J. Sci. Comput., 29(3), 1338–1354. (2007)
- [7] M. -J. Lai, On Construction of Bivariate and Trivariate Vertex Splines on Arbitrary Mixed Grid Partitions, Dissertation, Texas A&M University, 1989.
- [8] M. -J. Lai and Mersmann, C., Adaptive Triangulation Methods for Bivariate Spline Solutions of PDEs, Approximation Theory XV: San Antonio, 2016, edited by G. Fasshauer and L. L. Schumaker, Springer Verlag, (2017), pp. 155–175.
- [9] M. -J. Lai and L. L. Schumaker, Spline Functions over Triangulations, Cambridge University Press, 2007.
- [10] M. -J. Lai and L. L. Schumaker, Trivariate  $C^r$  polynomial macro-elements. Constr. Approx. 26 (2007), no. 1, 11–28.
- [11] M. -J. Lai and Wang, C. M., A bivariate spline method for 2nd order elliptic equations in non-divergence form, Journal of Scientific Computing , (2018) pp. 803–829.
- [12] M. -J. Lai and Y. Wang, Sparse Solutions to Underdetermined Linear Systems, Publication, Philadelphia (2021).
- [13] M. -J. Lai and Wenston, P., Bivariate Splines for Fluid Flows, Computers and Fluids, vol. 33 (2004) pp. 1047–1073.
- [14] J. Lee, A Multivariate Spline Method for Numerical Solution of Partial Differential Equations, Dissertation (under preparation), University of Georgia, 2022.

- [15] L. Mu and X. Ye, A simple finite element method for non-divergence form elliptic equations, *International Journal of Numerical Analysis and Modeling* 14(2)(2017), pp. 306–311.
- [16] L. L. Schumaker, *Spline Functions: Computational Methods*. SIAM Publication, Philadelphia (2015).
- [17] L. L. Schumaker, Solving elliptic PDE's on domains with curved boundaries with an immersed penalized boundary method. *J. Sci. Comput.* 80 (2019), no. 3, 1369–1394.
- [18] I. Smears, and E. Süli, Discontinuous Galerkin finite element approximation of nondivergence form elliptic equations with Cordes coefficients. *SIAM J. Numer. Anal.* 51(4), 2088–2106 (2013).
- [19] C. Wang, J. Wang, A primal dual weak Galerkin finite element method for second order elliptic equations in non-divergence form, *Math. Comp.*, 2019.

## 9 Appendix: Convergence of Algorithm 1

In this section, we first explain Algorithm 1 which is used to solve the minimization problem (16). In fact, Algorithm 1 is derived based on the solution to the following minimization

$$\min_{\mathbf{c}} J(c) = \frac{1}{2}(\alpha\|B\mathbf{c} - \mathbf{g}\|^2 + \beta\|H\mathbf{c}\|^2 + \gamma\|H_0\mathbf{c}\|^2) \quad \text{subject to } -K\mathbf{c} = \mathbf{f}, \quad (36)$$

where  $B, \mathbf{g}$  are associated with the boundary condition,  $H$  is associated with the smoothness condition  $\alpha > 0, \beta > 0$  are fixed parameters. Let us give a reason why we use (36) to replace (16). By Lemma 2, we know spline functions can approximate the solution of the PDE very well when the solution  $u$  is in  $H^3(\Omega)$ . When the size  $|\Delta|$  is small enough, for the quasi-interpolatory spline  $S_u$  can approximate  $u$  such that  $\|\Delta(u - S_u)\|_{L^2(\Omega)} \leq \epsilon_1$ . That is, the feasible set of (16) is not empty. We thus seek a spline solution  $u_s$  satisfying (36).

We use the similar technique in [1]. For convenience, we first consider the problem

$$\min_{\mathbf{z}} J(c) = \frac{1}{2}(\alpha\|B\mathbf{z} - \mathbf{g}\|^2 + \beta\|H\mathbf{z}\|^2) \quad \text{subject to } -K\mathbf{z} = \mathbf{f}, \quad (37)$$

where  $B, \mathbf{g}$  are from the boundary condition,  $H$  is from the smoothness condition. By the theory of Lagrange multipliers, letting

$$\mathcal{U}(z, \lambda) = \frac{1}{2}(\alpha z^\top B^\top B z - \alpha z^\top B^\top G - \alpha G^\top B z + \alpha G^\top G + \beta z^\top H^\top H z) + \lambda^\top (Kz + \mathbf{f}),$$

there exist  $\lambda$  such that

$$\frac{\partial \mathcal{U}}{\partial z} = \alpha B^\top B z - \alpha B^\top G + \beta H^\top H z + K^\top \lambda = 0 \quad (38)$$

$$\frac{\partial \mathcal{U}}{\partial \lambda} = Kz + \mathbf{f} = 0 \quad (39)$$

We can rewrite above linear equations as follow:

$$\begin{bmatrix} K^\top & \alpha B^\top B + \beta H^\top H \\ O & K \end{bmatrix} \begin{bmatrix} \lambda \\ z \end{bmatrix} = \begin{bmatrix} \alpha B^\top G \\ -\mathbf{f} \end{bmatrix} \quad (40)$$

To solve (40), we consider the following sequence of problems for a fixed  $\epsilon > 0$ :

$$\begin{bmatrix} K^\top & \alpha B^\top B + \beta H^\top H \\ -\epsilon I & K \end{bmatrix} \begin{bmatrix} \lambda^{(k+1)} \\ z^{(k+1)} \end{bmatrix} = \begin{bmatrix} \alpha B^\top G \\ -\mathbf{f} - \epsilon \lambda^{(k)} \end{bmatrix} \quad (41)$$

for  $k = 0, 1, \dots$ , with an initial guess  $\lambda^{(0)} = 0$ . Note that (41) reads

$$\begin{aligned} (\alpha B^\top B + \beta H^\top H)z^{(k+1)} + K^\top \lambda^{(k+1)} &= \alpha B^\top G \\ Kz^{(k+1)} - \epsilon \lambda^{(k+1)} &= -\mathbf{f} - \epsilon \lambda^{(k)} \end{aligned}$$

Multiplying on the both sides of the second equation in (41) by  $K^\top$ , we get

$$K^\top Kz^{(k+1)} - \epsilon K^\top \lambda^{(k+1)} = -K^\top \mathbf{f} - \epsilon K^\top \lambda^{(k)}$$

or

$$K^\top \lambda^{(k+1)} = \frac{1}{\epsilon} K^\top Kz^{(k+1)} - \frac{1}{\epsilon} K^\top \mathbf{f} + K^\top \lambda^{(k)}$$

and substitute it into the first equation in (41) to get

$$(\alpha B^\top B + \beta H^\top H)z^{(k+1)} + \frac{1}{\epsilon} K^\top Kz^{(k+1)} - \frac{1}{\epsilon} K^\top \mathbf{f} + K^\top \lambda^{(k)} = \alpha B^\top G.$$

Simplifying the above equation leads to

$$(\alpha B^\top B + \beta H^\top H + \frac{1}{\epsilon} K^\top K)z^{(k+1)} = \alpha B^\top G + \frac{1}{\epsilon} K^\top \mathbf{f} - K^\top \lambda^{(k)} \quad (42)$$

It follows that

$$z^{(1)} = (\alpha B^\top B + \beta H^\top H + \frac{1}{\epsilon} K^\top K)^{-1} (\alpha B^\top G + \frac{1}{\epsilon} K^\top \mathbf{f} - K^\top \lambda^{(0)}) \quad (43)$$

Using the first equation in (41), i.e.,  $(\alpha B^\top B + \beta H^\top H)z^{(k+1)} = \alpha B^\top G - K^\top \lambda^{(k+1)}$  to replace  $\alpha B^\top G$  in (42), we have

$$(\alpha B^\top B + \beta H^\top H + \frac{1}{\epsilon} K^\top K)z^{(k+1)} = (\alpha B^\top B + \beta H^\top H)z^{(k)} + \frac{1}{\epsilon} K^\top \mathbf{f}. \quad (44)$$

We get the minimizer using (43) and (44). These lead to Algorithm 1.

Next we show the convergence of the above iterative algorithm. Since the minimization problem (16) is convex over a convex feasible set, we know that the minimization has a unique solution. We may assume that the linear system from Lagrange multiplier method has a solution pair  $(\lambda, z)$  with a unique solution  $z$  if the size  $|\Delta|$  of triangulation  $\Delta$  is small enough and the spline space  $S_D^r(\Delta)$  is dense enough in  $H^2(\Omega) \cap H_0^1(\Omega)$ .

**Theorem 13** *Suppose that the matrices  $K, H, B$  satisfy the following consistent condition: if  $Kz = 0, Hz = 0$ , and  $Bz = 0$ , one has  $z = 0$ . Then there exists a constant  $\tilde{C}(\epsilon)$  depending on  $\epsilon$  but independent of the iteration number  $k$  such that*

$$\|z^{(k+1)} - z\| \leq \|\tilde{K}^{-1}\| \|K^\top\| \left( \frac{\tilde{C}\epsilon}{1 + \tilde{C}\epsilon} \right)^{k+1}$$

for  $k \geq 1$ , where  $\tilde{C} = \|K^+\|^2 \|\alpha B^\top B + \beta H^\top H\|$  and  $K^+$  stands for the pseudo inverse of  $K$  and  $\tilde{K} = \alpha B^\top B + \beta H^\top H + \frac{1}{\epsilon} K^\top K$ .

*Proof.* First, we show that  $\tilde{K}$  is invertible for  $\alpha, \beta > 0$ . If  $\tilde{K}z = 0$ , we have

$$c^\top \tilde{K}c = \alpha \|Bc\|^2 + \beta \|Hc\|^2 + \frac{1}{\epsilon} \|Kc\|^2 = 0$$

which implies that  $Kz = 0, Hz = 0, Bz = 0$ . By the assumption,  $z = 0$ . Thus,  $\tilde{K}$  is invertible and hence the sequence  $\{z^{(k)}\}$  is well-defined. Let  $\tilde{C}_1 = \|\tilde{K}\|$  which depends on  $\epsilon$ . From (40) and (42) ,

$$\begin{aligned}\tilde{K}z^{(k+1)} &= \alpha B^\top G + \frac{1}{\epsilon} K^\top \mathbf{f} - K^\top \lambda^{(k)} \\ \tilde{K}z &= \alpha B^\top G + \frac{1}{\epsilon} K^\top \mathbf{f} - K^\top \lambda.\end{aligned}$$

Hence, we have

$$z^{(k+1)} - z = \tilde{K}^{-1} K^\top (\lambda - \lambda^{(k)}). \quad (45)$$

By using (41) and (42), we get

$$-\epsilon(\lambda^{(k+1)} - \lambda) = -\epsilon(\lambda^{(k)} - \lambda) - \mathbf{f} - Kz^{(k+1)}$$

and

$$z^{(k+1)} = \tilde{K}^{-1} (\alpha B^\top G + \frac{1}{\epsilon} K^\top \mathbf{f} - K^\top \lambda^{(k)}).$$

It follows that

$$\begin{aligned}-\epsilon(\lambda^{(k+1)} - \lambda) &= -\epsilon(\lambda^{(k)} - \lambda) - \mathbf{f} - Kz^{(k+1)} \\ &= -\epsilon(\lambda^{(k)} - \lambda) - \mathbf{f} - K\tilde{K}^{-1} (\alpha B^\top G + \frac{1}{\epsilon} K^\top \mathbf{f} - K^\top \lambda^{(k)}) \\ &= -\epsilon(\lambda^{(k)} - \lambda) - \mathbf{f} - K\tilde{K}^{-1} (\tilde{K}z + K^\top \lambda - K^\top \lambda^{(k)}) \\ &= -\epsilon(\lambda^{(k)} - \lambda) - \mathbf{f} - Kz - K\tilde{K}^{-1} K^\top (\lambda - \lambda^{(k)}).\end{aligned}$$

As a result, we get

$$(\lambda^{(k+1)} - \lambda) = (\lambda^{(k)} - \lambda) (I - \frac{1}{\epsilon} K\tilde{K}^{-1} K^\top). \quad (46)$$

In order to show the next step, we use Lemma 7 in [1], i.e.,  $\mathbb{R}^m = \text{Ker}(K^\top) \oplus \text{Im}(K)$  where  $\text{Ker}(K^\top)$  is the kernel of  $K^\top$ . Assume that  $\lambda \in \text{Im}(K)$ . By the second equation in (41) that

$$K(z^{(k+1)} - z) = \epsilon(\lambda^{(k)} - \lambda^{(k+1)}).$$

That is,  $\lambda^{(k)} - \lambda^{(k+1)}$  is in the  $\text{Im}(K)$  and therefore

$$\lambda^{(k)} - \lambda = \sum_{j=1}^k (\lambda^{(j)} - \lambda^{(j-1)}) + (\lambda^{(0)} - \lambda),$$

we have  $\lambda^{(k)} - \lambda \in \text{Im}(K)$  for each  $k$ . From (46), we need to estimate the norm of  $I - \frac{1}{\epsilon} K \tilde{K}^{-1} K^\top$  restricted to  $\text{Im}(K)$  in order to estimate the norm of  $\lambda^{(k+1)} - \lambda$ . We write  $\|I - \frac{1}{\epsilon} K \tilde{K}^{-1} K^\top\|$  for  $\|(I - \frac{1}{\epsilon} K \tilde{K}^{-1} K^\top)|_{\text{Im}(K)}\|$  and we have:

$$\|\lambda^{(k+1)} - \lambda\| \leq \|I - \frac{1}{\epsilon} K \tilde{K}^{-1} K^\top\| \|\lambda^{(k)} - \lambda\|.$$

We claim that

$$\|I - \frac{1}{\epsilon} K \tilde{K}^{-1} K^\top\| \leq \frac{\tilde{C}_2 \epsilon}{1 + \tilde{C}_2 \epsilon},$$

for some constant  $\tilde{C}_2 > 0$ . Indeed, by the Rayleigh-Ritz quotient, we have

$$\|\lambda^{(k+1)} - \lambda\| \leq \|I - \frac{1}{\epsilon} K \tilde{K}^{-1} K^\top\| = \max_{0 \neq v \in \text{Im}(K)} (1 - \frac{1}{\epsilon} \frac{v^\top K \tilde{K}^{-1} K^\top v}{v^\top v}).$$

By using a technique from [1], we can get

$$\frac{1}{\epsilon} \frac{v^\top K \tilde{K}^{-1} K^\top v}{v^\top v} > \frac{1}{1 + \tilde{C}_2 \epsilon}, \quad \forall v \in \text{Im}(K)$$

where  $\tilde{C}_2 = \|K^+\|^2 \|\alpha B^\top B + \beta H^\top H\|$ . It follows that

$$\|I - \frac{1}{\epsilon} K \tilde{K}^{-1} K^\top\| \leq 1 - \frac{1}{1 + \tilde{C}_2 \epsilon} = \frac{\tilde{C}_2 \epsilon}{1 + \tilde{C}_2 \epsilon}.$$

As a results, we obtain

$$\|\lambda^{(k+1)} - \lambda\| \leq \frac{\tilde{C}_2 \epsilon}{1 + \tilde{C}_2 \epsilon} \|\lambda^{(k)} - \lambda\|$$

and from (45)

$$\|z^{(k+1)} - z\| \leq \|\tilde{K}^{-1}\| \|K^\top\| \left( \frac{\tilde{C}_2 \epsilon}{1 + \tilde{C}_2 \epsilon} \right)^{k+1} \|\lambda^{(0)} - \lambda\|.$$

□